Carbon Neutralization

WILEY

Carbon Neutralization

REVIEW OPEN ACCESS

Research Progress on Radiation Volt-Effect Isotope Cells

Qiannan Zhao[1] | Zhenxuan Liu[1] | Kai Huo[1] | Wenguang Zhang[1] | Bo Xiao[1] | Yuchen Xiong[1,2] | Yihuai Huang[1] | Changkai Huang[1] | Yao Luo[3] | Yan Liu[3] | Li Wang[4] | Abdul Basit[5] | Guibin Shen[6] | Yubo Luo[1] | Qinghui Jiang[1] | Xin Li[1,7] | Junyou Yang[1]

[1]State Key Laboratory of Materials Processing and Die & Mould Technology, School of Materials Science and Engineering, Huazhong University of Science and Technology, Wuhan, China | [2]China-Eu Institute for Clean and Renewable Energy, Huazhong University of Science and Technology, Wuhan, China | [3]China Nuclear Power Operation Technology Corporation, Ltd., Wuhan, China | [4]School of Photovoltaic and Renewable Energy Engineering, University of New South Wales, Sydney, New South Wales, Australia | [5]Department of Applied Physics, The Hong Kong Polytechnic University, Kowloon, Hong Kong, China | [6]School of Electrical and Electronic Engineering, Nanyang Technological University, Singapore, Singapore | [7]Guangdong HUST Industrial Technology Research Institute, Guangdong Provincial Key Laboratory of Manufacturing Equipment Digitization, Dongguan, Guangdong, China

Correspondence: Xin Li (xin_li@hust.edu.cn) | Junyou Yang (jyyang@mail.hust.edu.cn)

Received: 5 June 2025 | **Revised:** 14 July 2025 | **Accepted:** 24 July 2025

Funding: This study was supported by the National Natural Science Foundation of China (Grant no. 62304082), Guangdong Basic and Applied Basic Research Foundation (Grant no. 2024A1515110044), the National Key Research and Development Program of China (Grant no. 2020YFA0715000), and the Natural Science Foundation of Hubei Province (Grant no. 2023AFB087).

Keywords: betavoltaic cell | energy conversion material | radioisotope batteries | wide bandgap semiconductor

ABSTRACT

Radioisotope batteries, as a highly efficient and long-lasting micro-energy conversion technology, demonstrate unique advantages in fields, such as aerospace, medical devices, and power supply in extreme environments. This paper provides a systematic review of the research progress in radioisotope batteries, with a focus on analyzing the performance of different semiconductor materials in terms of energy conversion efficiency, radiation resistance, and application potential. The content covers optimization strategies and application prospects for traditional and wide/ultra-wide bandgap semiconductor materials (including silicon, gallium arsenide, silicon carbide, gallium nitride, titanium dioxide, zinc oxide, diamond, gallium oxide, and perovskite, among others). It also identifies current technical challenges, including low energy conversion efficiency, accelerated performance degradation of semiconductor materials under irradiation, and challenges related to the safe management of radioisotope. Finally, the article outlines future research directions, emphasizing the promotion of practical applications of radioisotope batteries through material innovation, structural design, and process optimization, with the aim of advancing academic innovation and engineering practices to address extreme environmental conditions and long-term energy demands.

1 | Introduction

The rapid development of the economy is often accompanied by energy consumption. While fossil fuels, as the primary nonrenewable energy sources, have created significant value for humanity, they have also led to environmental pollution and energy shortages. Therefore, optimizing the energy structure, reducing dependence on fossil fuels, and developing new energy sources have become urgent needs for achieving sustainable development. Energy plays an indispensable role in modern society, spanning power generation, healthcare, transportation, communication, manufacturing, scientific equipment, deep-sea and space exploration, and Micro-Electro-Mechanical Systems (MEMS).

Qiannan Zhao, Zhenxuan Liu and Kai Huo contributed equally to this study.

MEMS refers to independent intelligent systems with overall dimensions on the millimeter scale or smaller, primarily comprising micro-sensors, micro-actuators, and micro-energy sources. With the rapid growth of the MEMS market in recent years, MEMS has found widespread applications in aerospace, defense, deep-sea and polar exploration, and industrial and agricultural sectors. Thanks to advancements in nanomaterials, MEMS dimensions have reached the millimeter or even micrometer scale. The highly integrated system structure at such small scales imposes higher demands on the design and fabrication of internal components. However, without a micro-energy source matching the system's size, the development of MEMS will be constrained. Thus, the pursuit and development of micro-energy sources with high volumetric power density compatible with these systems is imperative.

Compared with traditional miniature batteries, such as miniature zinc-nickel batteries, whose sealing problem is difficult to be solved effectively; miniature lithium batteries, which need to be recharged many times and are not highly practical [1]; and miniature solar batteries that can't be used in closed and lightless environments, radioisotope batteries have become a hot spot of research in the field of miniature energy because of their high energy density, long service life, wide temperature range and stable operation, and have a unique advantage in the fields of deep-space exploration, deep-sea detection, and power supply in remote areas. Detection and power supply in remote areas and other fields have unique advantages. It is worth noting that radioisotope batteries refer to a device that converts the energy released by the decay of radioactive isotopes into electrical energy. Based on the conversion mechanism, it can be divided into direct conversion mechanisms and indirect conversion mechanisms. Direct conversion types refer to radiation voltaic effect isotope batteries, including betavoltaic batteries, alphavoltaic batteries, and gammavoltaic batteries. Radiation voltaic effect isotope batteries utilize particles released during the decay of radioactive isotopes to directly generate current through the P–N junction of semiconductor materials. Compared with other conversion mechanisms, it has the unique advantages of high conversion efficiency, compact structure, small size, light weight, and strong environmental adaptability. Indirect conversion mechanisms include radioisotope thermoelectric generators (RTGs) and radioisotope photovoltaic batteries. RTGs utilize the thermal energy generated by the decay of radioactive isotopes, converting it into electrical energy through thermoelectric materials (thermocouples). The radioisotope photovoltaic battery first uses the energy released by isotope decay to excite fluorescent materials (such as phosphors), which then can generate electricity through photovoltaic cells. Broadly speaking, nuclear batteries encompass all devices that generate electricity using nuclear energy (including fission, fusion, or isotope decay), including isotope batteries and fission batteries. However, in practical applications, they are often used interchangeably with isotope batteries because current miniaturization technology primarily relies on isotope decay. The term “nuclear battery” as used in the following text refers specifically to radioisotope batteries. Figure 1a–e shows the physical drawings of micro-

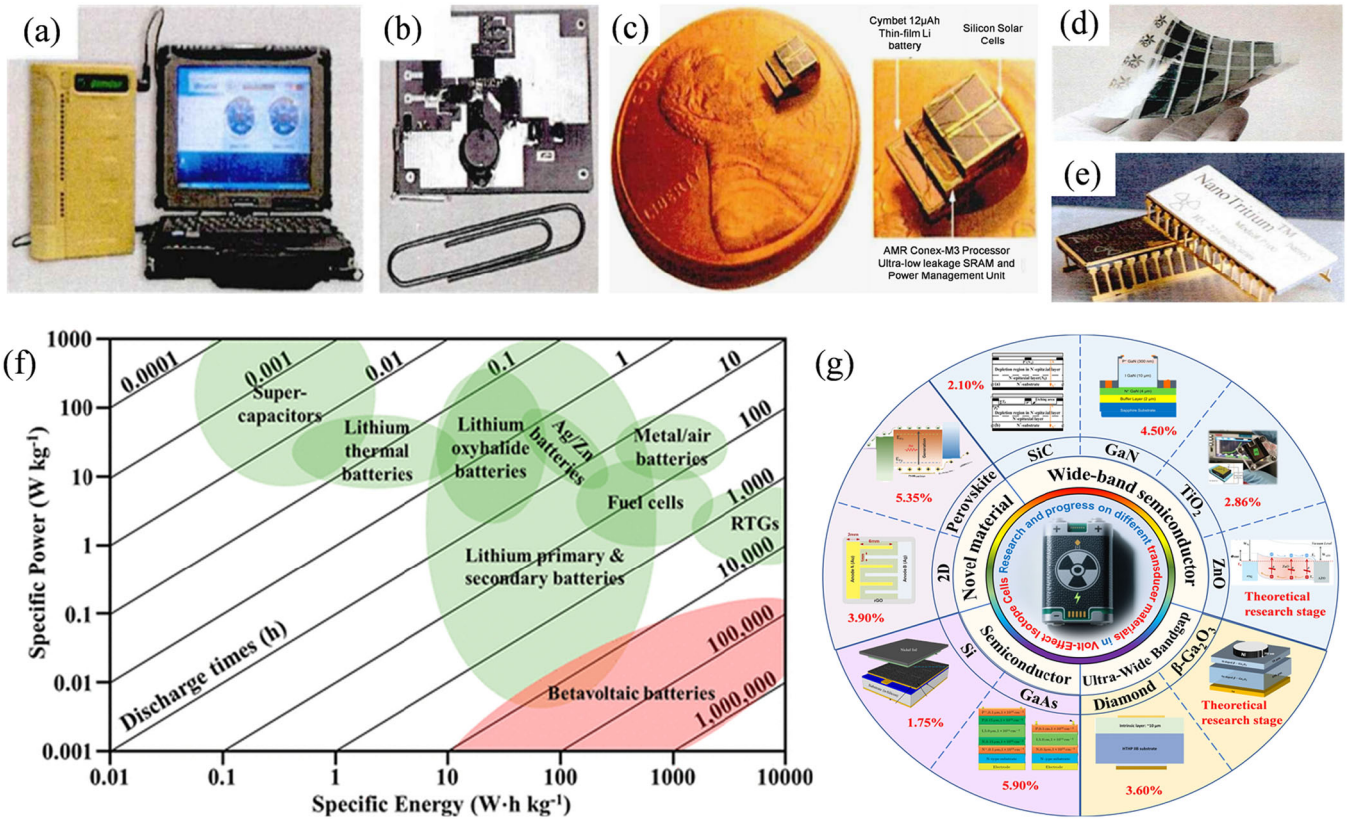

FIGURE 1 | (a) Pocket PC with micro-fuel cell. (b) Micro-fuel cell base unit. Reproduced with permission: Copyright 2007, Elsevier [2]. (c) Physical diagram of millimeter-scale energy autonomous sensor system with micro-lithium battery. Reproduced with permission: Copyright 2023, Springer Nature [3]. (d) Physical diagram of ultra-thin organic photovoltaic module from MIT. Reproduced with permission: Copyright 2022, John Wiley and Sons [4]. (e) Physical diagram of commercial micro-^{3}H nuclear battery from City Labs. (f) Specific energy of electrochemical batteries, supercapacitors, RTG and radiation voltaic effect isotope batteries battery specific energy. (g) Full-text overview diagram.

fuel cells, micro-lithium batteries, micro-photovoltaic batteries, and micro-tritium(^{3}H)nuclear batteries are shown, respectively. In addition, the specific energy density of radioisotope sources (e.g., ^{3}H, Nickel-63 (^{63}Ni), promethium-147 (^{147}Pm)) is much higher than that of conventional batteries, as shown in Figure 1f.

Since Rappaport's [5] first public demonstration of a radiation voltaic battery in 1954 using strontium-90/yttrium-90(^{90}Sr/^{90}Y) and a silicon (Si)-based P–N junction, experimental and theoretical research on such batteries has deepened. In 1973, Olsen [6] proposed the concept of betavoltaic batteries, achieving a maximum efficiency of 0.77% through experiments coupling Si-based P–N junction devices with a ^{147}Pm source. Theoretical models were also developed to calculate the limiting efficiencies of various semiconductor materials. As shown in Table 1. In 1976, Manasse et al. [22] introduced a Schottky junction betavoltaic batteries using ^{147}Pm, marking the first application of Schottky barriers in this field and broadening the range of semiconductor materials. Since then, with advancements in semiconductor fabrication, the power and efficiency of radiation voltaic isotope batteries have steadily improved, though they remain far from their theoretical limits.

In today's world, the escalating global climate crisis and the growing severity of carbon emissions have made the unsustainability of traditional fossil fuels and the environmental issues they pose the primary obstacles to achieving carbon neutrality goals. To meet these goals, there is an urgent need to develop new low-carbon auxiliary energy technologies for special application scenarios where renewable energy cannot fully cover the demand. Radiosotope batteries offer unique advantages such as zero operational carbon emissions, an ultra-long lifespan (up to several decades), and maintenance-free operation. They can effectively replace traditional high-carbon footprint power sources like diesel generators and frequently replaced chemical batteries, thereby significantly reducing carbon emissions across the entire lifecycle. Compared to energy storage technologies like lithium-ion batteries that rely on high-energy-consuming mineral extraction, this technology not only reduces the generation of electronic waste but also enables the resource utilization of nuclear waste, providing an important supplement to the construction of a diversified carbon-neutral energy system. Although some progress has been made in this field in the past few decades, there are still a series of key scientific and technical bottlenecks that need to be broken through: first, the current actual conversion efficiency of radiosotope batteries is usually much lower than the theoretical value, which seriously restricts their ability to supply energy in real microsystems; second, long-term irradiation of high-energy particles is prone to radiation damage of semiconductor materials, resulting in the degradation of battery performance over time, which limits the actual life and reliability of the battery. Kim et al. [23, 24] summarized the effects of different types of radiation on the properties of β-Ga_2O_3. For example, under α-particle irradiation at 18 MeV, the carrier mobility of β-Ga_2O_3 decreased significantly, with a carrier removal factor ranging from 406 to 728 cm^{-1}. The carrier removal factor is a physical quantity that describes the extent of carrier concentration reduction in semiconductor materials caused by a unit dose of radiation particles in a radiation environment. Kirmani et al. [25] revealed the radiation damage and repair mechanisms in halide perovskites through energy-tuned dual irradiation doses. After irradiation with 0.06 MeV low-energy protons, the photoelectric conversion efficiency (PCE) decreased by 26%. Following secondary irradiation with 1.0 MeV high-energy protons, the PCE recovered slightly, indicating partial performance restoration. In addition, There are huge differences in the cost and difficulty of preparing different semiconductor materials, and existing research lacks systematic comparisons of material properties and comprehensive performance evaluations. Finally, the management of radioactive sources, manufacturing costs, and long-term safety issues associated with radiosotope batteries pose significant obstacles to their widespread application and industrialization in practical use. Therefore, this paper aims to provide an in-depth summary of the research progress on radiosotope batteries based on various materials, focusing on the optimization of conversion device materials and fabrication, device performance, and stability. Additionally, we offer insights into future directions for this field, with the ultimate goal of advancing the continuous progress and practical application of radiosotope batteries. For ease of reading, we have drawn a summary diagram of the entire text, as shown in Figure 1g.

2 | Principles of Operation

2.1 | Basic Working Mechanism and Energy Conversion of Radiation Voltaic Effect Isotope Batteries

The working principle of radiation voltaic batteries involves the decay of radioactive isotopes, which releases radiation to bombard semiconductor conversion devices, generating a large number of electron–hole pairs (EHPs). These EHPs are separated by the built-in electric field, undergoing drift, diffusion, and recombination, thereby producing radiation current (J_β) and forward current (J_F). Ultimately, these currents are transmitted to external circuits via electrodes, converting decay energy into electrical energy, as shown in Figure 2a.

In radiation voltaic batteries, the process of generating and outputting electrical energy involves the generation and transportation of J_β and diode forward current, as well as the process of outputting electrical energy from the external load. The specific processes include: (1) Generation of radiation current. (2) Generation and transportation of diode forward current: The P–N junction or Schottky junction in radiation voltaic batteries plays the role of rectification, as shown in Figure 2b,c, to ensure that only the forward current passes through. When the battery is connected to an external load, the forward current flows partially through the diode to the external load. (3) Output power from external load: The size of the battery output current (current flowing through the load) and output voltage (voltage of the external load) depends on the magnitude of the radiated current and the forward current of the diode. The generation of radiated current is affected by the intensity of particles released by the radioactive source and the characteristics of the semiconductor material; while the size of the diode forward current depends on the characteristics of the P–N junction and the resistance of the external load.

TABLE 1 | Summary of conversion efficiencies for various materials.

Transducer material	Year	Bandgap (eV)	Radiation source	Short-circuit current (nA)	Open-circuit voltage (V)	Max output power (nW)	Efficiency (%)	Ref
Si	1953	1.12	$^{90}Sr/^{90}Y$	100	0.25	800	0.4	[5]
	2007		^{147}Pm	550	0.11	44	1.75	[7]
GaAs	2020	1.42	^{3}H	760	0.91	560	5.9	[8]
SiC	2006	2.9	^{63}Ni	41.9	0.72	6.17	1.2	[9]
	2011		^{63}Ni	12.75	0.98	8	1.99	[10]
	2024		He ion electrostatic gas pedal (simulated α)	591.34	1.87	406.66	2.1	[11]
GaN	2011	3.39	^{63}Ni	89.2	0.14	1.75	1.6	[12]
	2011		^{63}Ni	16	1.62	14.3	1.13	[13]
	2015		^{63}Ni	0.57	1.64	0.93	0.98	[14]
	2023		He ion electrostatic gas pedal (simulated α)	86.8	1.13	67.91	4.50%	[15]
Diamond	2018	5.47	^{63}Ni	6.35	1.02	4.65	1.25	[16]
	2015		^{63}Ni	55	1.68	45	0.6	[17]
	2015		^{238}Pu	2400	1.81	2400	3.6	[17]
	2024		Electron gun (β)	/	0.8	166	3.19	[18]
Perovskite	2021	2.3	15 keV electron beam (simulated β)	1541.22	1.28	1203	5.35	[19]
	2022	1.5	He ion electrostatic gas pedal (simulated α)	42.93	0.498	130.71	0.886	[20]
	2024	1.2–2.3 eV	$^{243}Am(\alpha)$	20.4	0.2	1.53	0.889	[21]

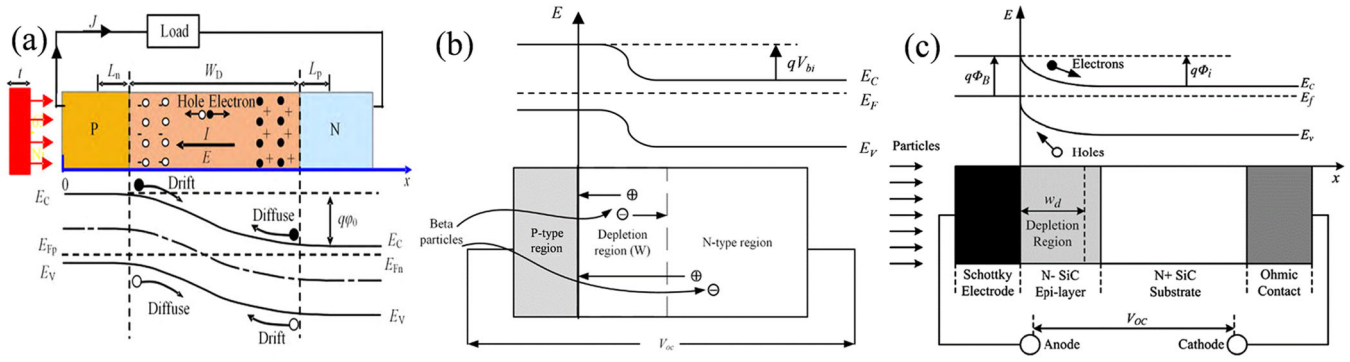

FIGURE 2 | (a) Working principle and energy band diagram of the conversion device. (b) Schematic of betavoltaic batteries based on a P–N junction. (c) Schematic of betavoltaic batteries based on a Schottky junction. Reproduced with permission: Copyright 2011, IEEE [26].

In an ideal diode, during battery operation, the direction of the radiation current is opposite to that of the P–N junction forward current. Under ideal conditions (neglecting depletion region recombination, surface recombination, and series/parallel resistance effects), the forward current equals the sum of electron and hole diffusion currents (J_D). The output current (J) is the difference between the radiation current and forward current ($J = J_\beta - J_F$), flowing from P to N. The output voltage corresponds to a forward bias applied to the P–N junction, reducing the barrier height to $q(\Phi_0 - V_{OC})$. The output power is $P = JV$. Under open-circuit conditions, the diffusion current cancels the radiation current, resulting in zero output current ($J = 0$). The output voltage in this state is termed the open-circuit voltage (V_{OC}). Under short-circuit conditions, the applied bias $V = 0$, the forward current $J_F = 0$, and the output current equals the radiation current ($J = J_\beta$), known as the short-circuit current (J_{SC}) and $J_{SC} = J_\beta$.

In summary, the radiation voltaic battery provides input energy to the transducer via a radioactive source, which is then converted into electrical energy by the transducer. The output performance of the radiation voltaic battery can be characterized by output current, output voltage, and output power. Among these, J_{SC}, V_{OC}, and maximum output power are key performance parameters of the radiation voltaic battery. Throughout the process, the interaction between the radiation current and the diode forward current determines the magnitude and stability of the output electrical energy. By controlling the activity of the radioactive source, optimizing the material parameters and structural design of the energy conversion device, and appropriately matching the external load, efficient energy conversion and stable output of the radiation voltaic battery can be achieved.

2.2 | Composition of Radiation Voltaic Batteries

The core components of radiation voltaic batteries include a radioactive source, semiconductor energy conversion devices, and electrodes with encapsulation structures. Research on radiation voltaic batteries spans decades, and these elements collectively influence the energy conversion efficiency (ECE, the efficiency with which isotope batteries convert radiant energy into electrical energy) and output power density of the battery.

2.2.1 | Selection of Radioactive Sources

Based on the type of radioactive isotopes, radiation voltaic batteries can be categorized into three types: betavoltaic batteries, alphavoltaic batteries, and gammavoltaic batteries. Their corresponding penetration capabilities are illustrated in Figure 3e.

In radiation voltaic batteries, the selection of an appropriate radioactive source is essential to enhance the output performance of the battery. The following factors need to be considered when selecting a radioactive source:

1. Consider the type of radiation from the source. Since gamma (γ)-rays have high penetrating ability, the rays cause strong irradiation damage to the device, which may affect the lifetime of the battery and the safety of the user. Therefore, the best radioisotopes for radiation voltaic batteries are pure beta decay radioisotopes, which do not produce additional X-rays during use (high-energy beta source outgoing particles accompanied by a small amount of X-rays produced) and are most conducive to radiation protection. Moreover, ^{3}H, carbon (^{14}C), ^{147}Pm and other β radiation sources emit particles with low energy, which is not easy to cause displacement damage to semiconductor materials.
2. Equilibrium half-life and specific power relationship. The longer the half-life of the radioactive source, the longer the continuous energy supply time, the longer the service life of the battery. However, the specific power of the source is inversely proportional to its half-life; the longer the half-life, the lower the specific power. Therefore, it is necessary to weigh the conflicting effects of service life and low specific power.
3. Consider the decay particle energy. The larger the average particle energy, the higher the EHP generation rate, and the higher the battery output power; however, too high a particle energy will cause serious lattice damage to the transducer devices, leading to deterioration of battery performance. The half-life determines the working life of the nuclear battery; the average and maximum energy of particles determines the output power of the nuclear battery, the cost and difficulty of obtaining it, and so on.

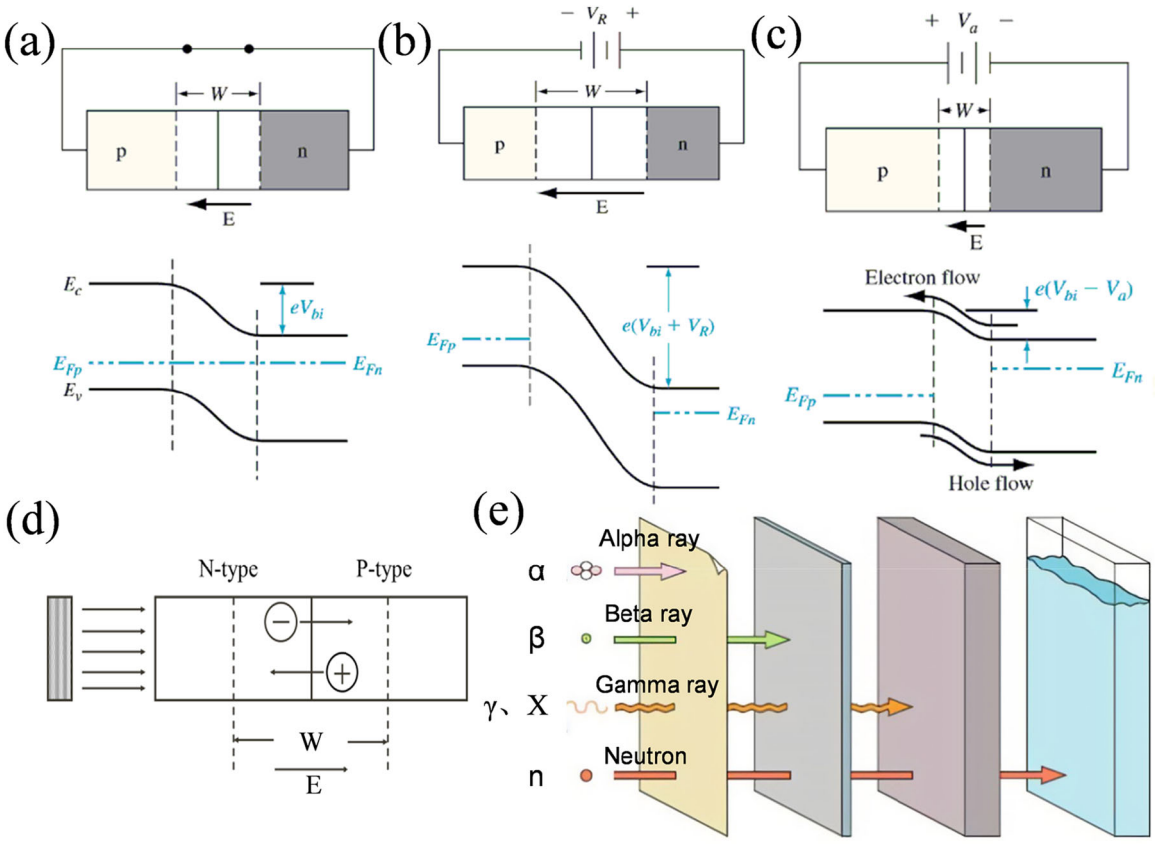

FIGURE 3 | Diagram of P–N junction and its associated energy bands: (a) zero bias, (b) reverse bias, (c) forward bias, (d) schematic diagram of the P–N junction transducer unit, and (e) penetration of α, β, and γ rays.

Currently, betavoltaic batteries are the smallest and most efficient type of isotope battery, they typically have higher energy densities and semiconductor efficiencies ranging from 1% to 20%, depending on the radioisotope and converter type.

2.2.2 | Semiconductor Energy Conversion Devices

In radiation voltaic batteries, the P–N junction serves as the conversion unit for separating EHPs. Figure 3a–c depicts the P–N junction and its energy band diagrams under zero bias, reverse bias, and forward bias, respectively, while Figure 3d illustrates the working principle of the P–N junction conversion unit.

In N-type semiconductors, electrons are majority carriers and holes are minority carriers; in P-type semiconductors, holes are the majority carriers, while electrons are the minority carriers. At the interface where the two are in contact, the holes in the P-region diffuse into the N-region and the electrons in the N-region diffuse into the P-region. Since the P- and N-regions are electrically neutral before the diffusion movement, after diffusion, the P-region is left with a negatively charged ionization acceptor and the N-region is left with a positively charged ionization donor. Thus, a space charge region, also called depletion region, is created at the interface of the P–N junction. In the depletion region, the negative charge in the P-region and the positive charge in the N-region form a built-in electric field, the direction points from the N region to the P region, Therefore, the EHPs separated in the depletion region drift into the P region, while the holes drift into the N region. When an EHP is generated inside the semiconductor material by the incidence of a radioactive source outgoing particle, it is separated in the depletion region and a current is generated. The minority carrier diffusion length in semiconductors refers to the average distance that minority carriers can travel within the material before recombination. In radioisotope batteries, when particles produce an excess of EHPs, they move through the depletion and neutral regions to be collected by the electrodes or to undergo complexation. The diffusion length is a key parameter in radioisotope batteries to quantify how far these carriers can travel before compounding. The diffusion length of a transducer device is affected by factors such as material type, doping level, presence of defects in the crystal, and temperature. For the transducer unit of a radioisotope battery, different semiconductor materials have different properties. Typically, we consider a longer minority carrier diffusion length to be advantageous because it means that β particles can better match the penetration depth for collecting EHPs, thereby fully utilizing the energy deposited by the radiation source within the semiconductor P–N junction.

2.2.3 | Electrodes and Encapsulation Structures

Electrodes and encapsulation structures are the key components of radioisotope batteries to realize efficient energy collection and safe operation, and their design has a direct impact on the output performance, lifetime, and reliability of the batteries. The core role of electrodes is to efficiently collect

separated electrons and holes in semiconductor transducer devices and transmit them to external circuits through low-resistance paths, and the choice of materials needs to take into account the conductivity and stability, for example, gold (Au) is commonly used in high-precision medical implantation equipment due to its high electrical conductivity and chemical stability, while aluminum (Al) is used in the large-area transducer devices of aerospace detectors due to its low-cost and easy-to-process characteristics. In terms of structural design, fork-finger electrodes can increase the contact area to enhance the collection efficiency, while multi-layer composite electrodes (e.g., Au/Ni/Si) can prolong the service life by combining the metal layer with the barrier layer. The encapsulation structure bears the dual task of radiation shielding and environmental protection, which needs to completely block the particles released by radioisotopes and resist external disturbances such as temperature and humidity, and so forth. Titanium alloys (lightweight and with high shielding efficiency) or ceramics (high-temperature and anti-irradiation) are often used as the materials, and the structural design realizes comprehensive protection through multilayered shielding (e.g., stainless steel outer layer and boron containing polyethylene inner layer) and thermal management (heat dissipating fins or heat-conducting silicone grease) to achieve comprehensive protection. In practice, NASA's RTG uses platinum electrodes and titanium encapsulation to provide power for the Mars rover, while medical pacemakers rely on gold electrodes and ceramic seals to ensure biosafety. In the future, with the breakthroughs in miniaturized packaging, self-repairing materials and biomimetic shielding design, the electrode and packaging technology will further promote the radioisotope batteries in the field of deep space exploration, medical, and other applications.

2.3 | Core Parameters of Radiation Voltaic Batteries

The performance of radiation voltaic batteries is mainly determined by key parameters, such as J_{SC}, V_{OC}, output power (P_{out}) and ECE, which are interrelated with each other and together determine the energy conversion capability of the battery.

J_{SC} is defined as the output current of the cell in short-circuit state, and its value is equal to the J_{β}, which directly reflects the number of carriers produced by the decay of radioisotopes, and the specific expression is as follows:

$$J_{SC} = \int_0^H qG(x)\mathrm{CE}(x)dx \tag{1-1}$$

where H is the thickness of the semiconductor in cm; q is the electron charge with a value of 1.60×10^{-19} C; x is the distance between the energy deposition location of the incident decay particle and the surface of the semiconductor in cm; $G(x)$ is the generation rate of EHPs; and $\mathrm{CE}(x)$ is the collection efficiency of EHPs. The J_{SC} can be increased by increasing the activity (A) of the radioactive source or selecting a high-energy radioactive source during optimization, but the contradiction between half-life and power density needs to be balanced.

The V_{OC} of a radiation voltaic battery is the maximum output voltage of the cell without load, which is closely related to the forbidden bandwidth (E_g) of the semiconductor material, and can be deduced from the J–V characteristic curve with the expression

$$V_{OC} = nV_T \ln\left(\frac{J_{SC}}{I_0} + 1\right) \tag{1-2}$$

where V_T is the thermal potential of the semiconductor, the value of $V_T = KT/q$; n is the device ideal factor, reacting to the P–N junction diffusion current and the proportionality of the composite current, generally take 1–2; I_0 is the reverse saturation current. The selection of wide-band materials (e.g., silicon carbide [SiC], gallium nitride [GaN]) for optimization can significantly improve the V_{OC}, because the forbidden band width is positively correlated with the V_{OC}, and the carrier complex loss is reduced by optimizing the P–N junction doping concentration.

The P_{out} of a radiation voltaic battery is affected by several factors such as the activity of the radioactive source, the average β-decay energy (E_{avg}, in eV), the source efficiency (η_s, the ratio of the energy exiting from the surface of the radioactive source to its total decay energy), the reflectance coefficient (r), and the device conversion efficiency (η_c, the device efficiency of the semiconductor transducer device), among which ηs and η_c are the key variables, and the former can be improved by the thin-film radiating source design to increase the ratio of particle ejection, while the latter relies on the enhancement of carrier collection efficiency and filling factor, and the following equation can express its correlation:

$$P_{out} = AE_{avg}\eta_s\eta_c = AE_{avg}\eta_s(1-r)\frac{QV_{OC}FF_q}{\varepsilon} \tag{1-3}$$

where Q is the carrier collection efficiency, V_{OC} is the open-circuit voltage (in V), FF is the fill factor, and is the average ionization energy (in eV). The device conversion efficiency can be expressed as $\eta_c = (1-r)QV_{OC}\mathrm{FF}_q/\varepsilon$, and the total energy conversion efficiency can be expressed as $\eta_{tot} = \eta_s\eta_c$.

Optimization principles include selecting semiconductor materials with long minority carrier diffusion lengths (such as high-purity Si) to enhance carrier collection, as well as reducing series resistance and optimizing junction doping concentrations to improve FF.

ECE is the core index for evaluating the comprehensive performance of the cell, and its optimization needs to integrate the matching of the radiation source and the transducer device, for example, for the alphavoltaic battery, the use of diamond semiconductors with strong resistance to radiation damage can achieve both high energy conversion and long service life; in addition, optimizing the battery structure (e.g., electrode layout, shielding thickness) through multiphysics simulation can further reduce the energy loss. In practice, we need to weigh the parameters according to the needs of the scenarios, such as deep space exploration, prioritizing long half-life radioactive sources

to ensure longevity, while military sensors require high specific power design to meet the demand for instantaneous power supply. In the future, through the combination of new semiconductor materials (e.g., 2D heterojunction), nanosizing of radioactive sources, and intelligent thermal management technologies, the performance of key parameters of radiation voltaic batteries is expected to achieve breakthroughs.

2.4 | Examples of Radioisotope Battery Applications

The core advantages of radioisotope batteries lie in their ultra-long lifespan, high energy density, and strong environmental adaptability (they are not affected by external conditions such as temperature and light), making them irreplaceable in extreme environments or long-term unmaintained settings. In the aerospace field, NanoTritium tritium batteries from the U.S.'s City Labs and Russia's ^{63}Ni batteries are used in CubeSat microsatellites and deep-space probes, respectively; in the military defense field, DARPA-funded betavoltaic micropower supplies provide long-lasting power for battlefield sensor networks and unmanned underwater equipment; and in the medical field, early isotope battery technology was used for pacemakers. In the 1970s, the Plutonium-238 (^{238}Pu) pacemaker produced by the U.S.-based company Medtronic provided more than 10 years of endurance, with about 3000 implantations around the globe. However, such applications were phased out of the market after the 1980s due to public concerns about radioactive materials and advances in lithium battery technology. In addition, these batteries have shown unique value in industrial monitoring, nuclear waste management and extreme environmental equipment. In the future, with the advancement of deep space exploration (e.g., lunar/Mars base construction) and deep sea development, as well as the application of wide-band semiconductor materials and new isotopes, the radioisotope batteries are expected to realize breakthroughs in a wider range of applications in the fields of deep space exploration, military equipment, and telemedicine.

3 | Semiconductor Material-Based Radiation Voltaic Batteries

3.1 | Silicon-Based Radiation Voltaic Battery

Single-crystal Si preparation and doping processes are mature and low-cost and have taken the lead as a transducer material for radiation voltaic batteries. Si-based radiation voltaic batteries are a type of isotope batteries utilizing silicon materials and the principle of the radiation voltaic effect. With the progress of research on radioactive energy, Si-based radiation voltaic batteries, as a new type of energy conversion device, has become the focus of research due to its high efficiency, long life, and wide application prospects.

The phenomenon of radioactive materials interacting with semiconductor materials to excite electrons and holes was proposed by Nevill Francis Mott as early as the 1960s [27]. This phenomenon is similar to the photovoltaic effect, but is driven by particles produced by radioactive decay rather than photons. Early research focused on verifying the fundamentals of this effect and finding suitable semiconductor materials. Researchers have found that silicon performs well as a semiconductor material in this type of radiation battery, offering high current output and stability [5].

In 1954, Rapport [5] successfully developed the world's first radiation voltaic battery by utilizing Sr^{90}/Y^{90} isotope source and Si semiconductor, and the output power of the battery was 0.8 nA cm^{-2} under the load resistance of 10 kΩ, and the energy conversion efficiency reached 0.4%. In the same year, Pfann et al. [28] conducted an in-depth research on ^{90}Sr/^{90}Y radiation voltaic battery. Battery conducted an in-depth study, deduced the maximum output power of the radiation voltaic battery and ECE of the formula, analyzed the performance parameters of the radiation voltaic battery and isotope source, semiconductor material selection of the relationship between, pointed out that the use of the Si semiconductor bandwidth is higher than the germanium (Ge) can be used to make the radiation voltaic battery has a higher output power.

Over the next two decades, research has focused on how to enhance the response of Si to radioactive particles by adjusting its doping, surface treatment,and so forth, to improve current output and energy conversion efficiency. To realize long-term remote power supply, Donald W. Douglas Laboratory [29, 30] designed and fabricated a series of prototype nuclear batteries using Si-based transducer devices and a ^{147}Pm radioactive source, the structure of which is shown in Figure 4a. This was the world's first successful commercialized betavoltaic battery with initial powers of 50, 200, and 400 μW. However, due to the large total activity of the sources used, which was prone to ^{147}Pm radiation contamination, its research was almost stagnant in the following decades. Until the 1990s, with the rapid development of MEMS and semiconductor field, the semiconductor preparation technology has been significantly improved, in the demand for independent miniature power supply traction, radiation voltaic batteries once again attracted the attention of researchers.

In 2011, Wu Kai et al. chose ^{63}Ni as the radioisotope-driven source and Si as the transducer material, and the maximum conversion efficiency was 5% after computational optimization [33]. Tang et al. conducted optimized design and analysis of batteries using Si-based ^{63}Ni isotope sources, incorporating considerations of isotope self-absorption effects. They simulated and calculated the transport process of particles in semiconductor materials using the Monte Carlo program (MCNP), and the optimal thickness of the isotope source and semiconductor material, the P–N junction depth of the semiconductor material, the thickness of the depletion region, the doping concentration, as well as the EHPs generated and collection were studied and analyzed, and the theoretical conversion efficiencies of 4.94% [32] and 13.49% [35] were obtained, respectively. Theoretically, the overall efficiency of betavoltaic batteries can be close to 7%–13.4%, but the actual demonstrated efficiency is not more than 2%. Sun et al. [36] developed a 63Ni-Si-based battery using a vertical sidewall square hole array energy conversion structure, which increased the surface area by more than 120% compared to

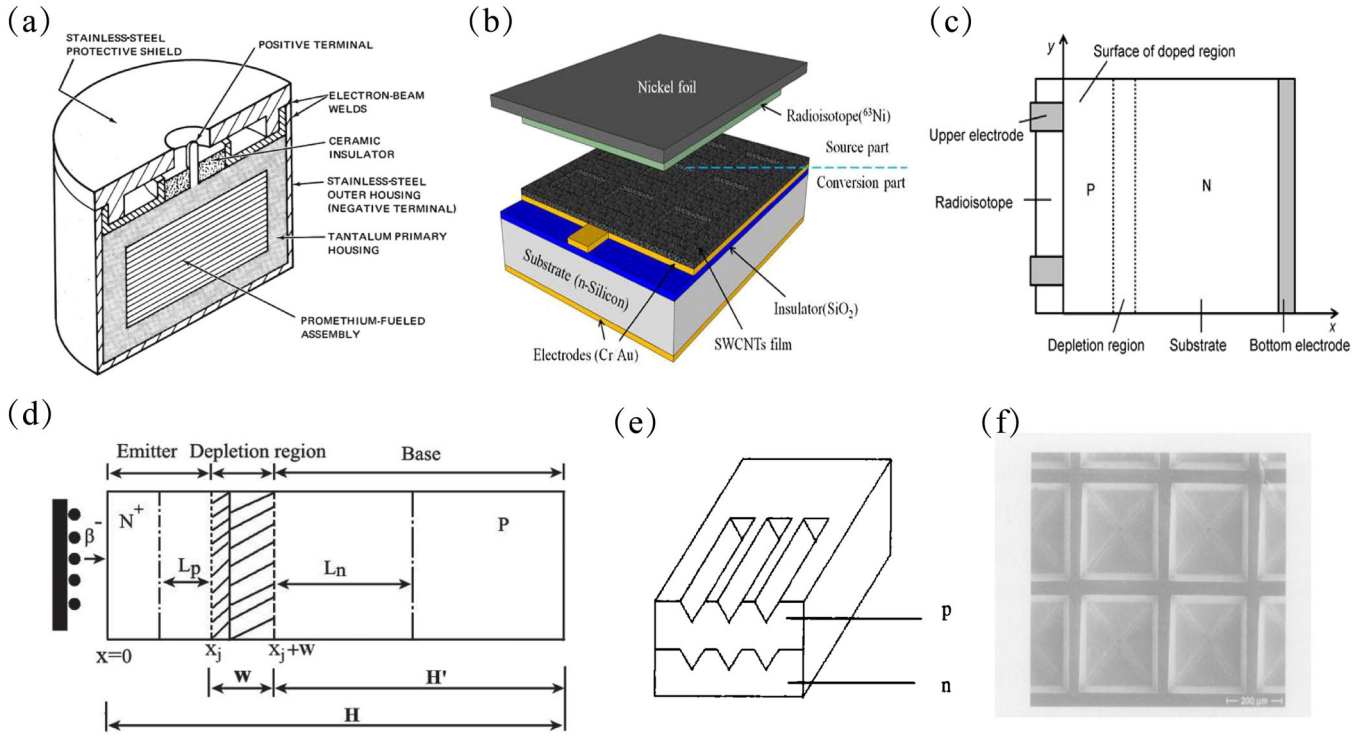

FIGURE 4 | (a) Betavoltaic cell structure using silicon-based sensor devices and ^{147}Pm radioactive sources. Reproduced with permission: Copyright 2017, Taylor and Francis [29, 30]. (b) Three-dimensional schematic of betavoltaic cell using single-walled carbon nanotubes (SWNTs)-silicon-based heterojunction structure. Reproduced with permission: Copyright 2014, Institute of Physics Publishing [31]. (c) Schematic of a planar betavoltaic cell. Reproduced with permission: Copyright 2012, Springer Nature [32]. (d) Schematic of a P–N junction silicon-based cell. Reproduced with permission: Copyright 2011, IEEE [33]. (e) Structure of a V-groove energy conversion. (f) Structure of an inverted pyramid energy conversion. Reproduced with permission: Copyright 2009, SPIE [34].

traditional energy conversion structures of the same size with openings of equal depth, such as inverted triangular straight slots or inverted pyramids. Additionally, the introduction of a new structure called the electroplating zone enhances the operational stability of the isotope microbattery, achieving a maximum output power of 0.79 nW mm^{-2}, though the conversion efficiency stands at 0.767%. Guo et al. [7] developed a new type of ^{147}Pm-Si based cell with a maximum output power of 4.89 nW mm^{-2} and a conversion efficiency of 1.75% by taking high-energy radioisotopes as the source and utilizing the mechanism of porous silicon to increase the energy gap and electron capture to improve the power output and energy conversion efficiency. Deus et al. [37] developed a betavoltaic battery for tritium power cells based on hydrogenated amorphous silicon NIP drift junctions with a ^{3}H (5 nm) metal contact layer. Amorphous silicon cells were exposed to a tritium gas atmosphere for 46 days and their performance was investigated over several time intervals, resulting in gaseous ^{3}H-a-Si (amorphous silicon)-based cells with a maximum output power of 1.36 nW mm^{-2} and a conversion efficiency of 1.2%. At present, the research on betavoltaic batteries is mainly for the study of source efficiency and conversion efficiency of the transducer chip, such as exploring and studying the structure of the radiation source material and attempting to use new types of transducer chips, new structures, and new materials, so as to increase ECE of the betavoltaic battery.

With advances in materials science and micro- and nanotechnology, researchers have been able to create more efficient prototype Si-based radiation voltaic batteries. These prototype cells used more advanced silicon nanostructures (e.g., nanowires, quantum dots, etc.) to improve radiation absorption efficiency and utilized more precise fabrication processes to reduce radiation damage. At this stage, the researchers focused on increasing the power density of the cells and addressing the energy loss and efficiency degradation that can occur during extended operation. To improve the energy conversion efficiency, some studies have also explored ways to composite Si with other materials (e.g., Ge, carbon nanotubes, etc.) to enhance the radiation absorption and charge separation efficiency. In 2014, Liu et al. [31] reported a betavoltaic battery using single-walled carbon nanotubes (SWNTs)-Si-based heterojunction structure, the structure of which is shown in Figure 4b. The one-dimensional structure of SWNTs substantially reduces carrier complexation and has high carrier mobility and very low carrier scattering. If a 3.3 mCi cm^{-2} ^{63}Ni source is used, a V_{OC} of 6.5 mV and a J_{SC} of 13 nA cm^{-2} with a conversion efficiency of 0.15% can be obtained, and its J_{SC} is 2000 times of the theoretical value, and the performance of this kind of cell can be further improved by further optimizing the design.

At the same time, relevant research has been carried out on the structural design of transducer devices and the influence of environmental factors in batteries. There are mainly three types of transducer device structures: flat plate, inverted pyramid, and V-groove. In 2002, Blanchard et al. [38] designed a Si-based transducer device with a V-groove structure; in 2003, Guo et al. [39] prepared a Si-based transducer device with an inverted pyramid structure; and in 2009, Chu et al. [34] compared the flat plate, the inverted pyramid, and the V-groove in Figure e.f.

The results showed that the output performance of the inverted pyramid and V-groove structures was superior to that of the flat plate.

Another important advance is how to repair damage to Si materials under long-term radiation exposure. By introducing advanced material repair techniques, it is possible to restore the electrical properties of the material to a certain extent and extend the service life of the battery. After entering the 2020s, with the advances in nanotechnology, microelectronics, and materials science, the energy conversion efficiency and stability of Si-based radiation voltaic batteries have been significantly improved. However, at present, from the reported Si-based betavoltaic battery, their energy conversion efficiency is still relatively low, mainly because of the narrow forbidden band width of Si materials, the larger leakage current of Si-based devices, and also their resistance to irradiation is still relatively poor, thus making it difficult to have a greater breakthrough in the output performance of Si-based radiation voltaic batteries.

Currently, silicon-based radiation voltaic batteries are widely recognized as an ideal power source for MEMS and sensors due to their tiny size and long-life characteristics. For example, in extreme environments (e.g., deep oceans, polar regions) or long-term unmaintained scenarios, such batteries can provide continuous power for temperature and pressure sensors. Medical devices such as pacemakers require a stable and long-lasting power source, and the long-life characteristics of batteries (e.g., ^{63}Ni half-life of 100 years) can significantly reduce the surgical risk of battery replacement, but the current power (in the microwatt class) still needs to be further enhanced to meet higher power consumption requirements. In conclusion, further breakthroughs in Si-based radiation voltaic batteries need to rely on new materials and structural innovations, while addressing regulatory, cost, and public acceptance issues. In the short term, its application will still focus on the special field; in the long term, if the power density and safety significantly improved or can be expanded to consumer electronics (such as Internet of Things devices) and other civilian scenarios.

It is worth noting that in the photovoltaic industry, crystalline silicon solar cells are developing rapidly, leading to a sharp increase in demand for Si wafers [40]. During the processing of silicon wafer preparation, approximately 30% of high-purity silicon (99.9999%) is lost through cutting into silicon slurry, resulting in waste silicon. High-value recycling of photovoltaic silicon waste is an important pathway to achieving "carbon neutrality." Therefore, recycling and purification technologies for photovoltaic industry waste silicon materials can be introduced as a low-cost silicon source to replace traditional high-purity silicon [41–44]. Future research will continue to focus on the development of new semiconductor materials, such as quantum dots, carbon nanotubes, and graphene, to improve the efficiency of radioisotope batteries. Advances in nanotechnology have allowed the structure and properties of these materials to be finely tuned, thus providing more innovative possibilities for radioisotope batteries. With the focus on environmental and safety issues, researchers are also looking for alternative less radioactive isotopes to minimize potential harm to the environment. In addition, more research is needed to improve the way radioisotopes are produced and stored to ensure the long-term safe operation of radioisotope batteries.

3.2 | Gallium Arsenide-Based Radiation Voltaic Battery

Compared with Si materials, gallium arsenide (GaAs) has higher electron mobility, better radiation resistance, and stronger radiation absorption, making it a potential as a semiconductor material in radiation voltaic batteries. GaAs is able to absorb high-energy particles more efficiently and convert them into electric currents. In 1964, Flicker et al. used a ^{147}Pm radioactive source in their study and the performance of the transducer materials was were compared [45]. In addition to Si and Ge, which were already widely used at that time, they introduced GaAs, which has a larger forbidden bandwidth and a higher radiation damage threshold. Theoretical calculations show that among the three materials, GaAs-based radiation voltaic batteries have the highest conversion efficiency. However, due to the immaturity of semiconductor material growth processes at the time, the minority carrier diffusion length of the GaAs-based P–N junction that could be produced was extremely short, and the carrier collection efficiency was extremely low, rendering it of no practical value. Therefore, no prototype was produced for performance comparison.

Initial studies focused on testing the radiative responsivity of GaAs materials, which showed that the theoretical value of energy conversion efficiency of GaAs-based betavoltaic batteries could reach up to 18.5% without considering isotope-derived absorption effects [46]. Chen et al. [47] designed and prepared GaAs-^{63}Ni-based radiation voltaic battery with PtP-N$^+$ junction by considering the effect of surface state density and minority carrier diffusion length, as shown in Figure 5c, and the optimized results obtained were $J_{SC} = 28$ nA cm^{-2} and $V_{OC} = 0.3$ V. Andreev et al. [52] prepared $Al_{0.35}Ga_{0.65}As$-^{3}H-based battery with an ECE of only 12% (the theoretical value is up to 23.5%), and all of these findings are far from the ideal value. The reason for this is that, in addition to the limitations of the existing semiconductor processing technology, isotope source loading technology, the optimal design of the physical parameters of the transducer unit is also an important influence factor. Experimental results show that GaAs is able to respond better to α and β particles, especially in the high-energy radiation environment shows good stability. Therefore, GaAs is beginning to be recognized as a promising material for radiation voltaic batteries.

In 2012, Li et al. [50] prepared GaAs-based P$^+$PINN$^+$ junction radioisotope cells as shown in Figure 5c by adding an intercalation layer to a typical PIN structure. The test results show that the ECE is 1.45 times higher than that of the conventional PIN structure, the reason is that the use of the P$^+$PINN$^+$ structure can increase the width of the space charge region in the cell and improve the collection efficiency of the minority carriers, and at the same time, the density of the lattice defects in the material will be reduced, and the minority carrier lifetime will be increased, which will ultimately improve the output performance of GaAs-based radioisotope cells. In 2015, Wang et al. [53] investigated the effect of ambient temperature on the output performance of ^{63}Ni-GaAs and ^{147}Pm-GaAs

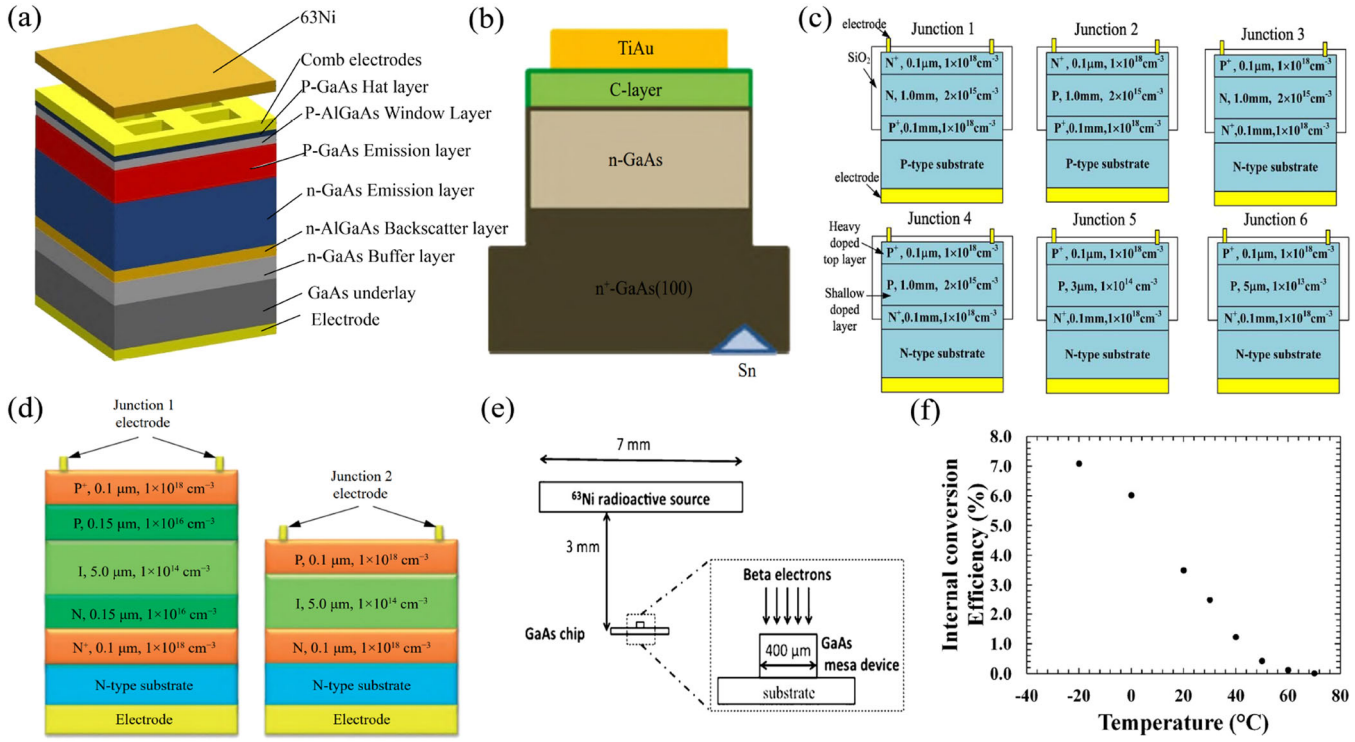

FIGURE 5 | (a) Schematic structure of GaAs-based betavoltaic battery. Reproduced with permission: Copyright 2022, IOP Publishing [48]. (b) GaAs-based Schottky-type isotope cell modified by depositing a carbon layer. Reproduced with permission: Copyright 2022, Elesvier [49]. (c) Schematic structure of GaAs-^{63}Ni-based isotope cell designed and prepared by Chen et al. employing a PtP-N^{+} junction. Reproduced with permission: Copyright 2022, IOP Publishing [47]. (d) GaAs-based P^{+}PINN^{+} junction and PIN junction type isotope cells. Reproduced with permission: Copyright 2012, IOP Publishing [50]. (e) Schematic geometry of GaAs-^{63}Ni betavoltaic battery. Reproduced with permission: Copyright 2017, Elesvier [51]. (f) Experimental maximum power versus temperature for GaAs-^{63}Ni betavoltaic battery. Reproduced with permission: Copyright 2017, Elesvier [51].

isotope cells. Their theoretical calculations and experimental test results showed that the cell V_{OC} and ECE increased with the temperature decrease, and the experimental measurements of the V_{OC} of ^{63}Ni-GaAs and ^{147}Pm-GaAs cells were 0.47 and 0.41 V, respectively, and the ECE could reach 0.44% and 0.11%, respectively, at 213.15 K. In 2017, Butera et al. [51] also investigated the effect of ambient temperature on the output performance of GaAs-based isotope cells, as shown in Figure 5f, where a maximum output power density of 1.4 nW cm^{-2} was obtained at −20°C (with a ^{63}Ni source activity of 172 MB$_q$).

Then researchers have begun to explore how to optimize the performance of GaAs materials. For example, doping, heterostructure design (e.g., GaAs/AlGaAs heterostructures), and surface treatment techniques are used to enhance the ECE and responsiveness to radiation of GaAs materials. In 2019, Khvostikov et al. [8] presented an AlGaAs/GaAs heterojunction-based commutation energy cell with an ECE of 5.9% under the irradiation of a tritium source. In 2022 Dorokhin et al. [49] reported a GaAs-based Schottky-type isotope cell modified by depositing a carbon layer, as shown in Figure 5b. Their experimental and simulation results showed that carbon deposition on the top of the n-GaAs layer can passivate its surface state, which is conducive to the improvement of the output performance of the cell. GaAs has a good absorption capacity of γ-rays and high-energy electrons, which makes the GaAs-based isotope cell have a significant advantage in some high-radiation environments.

The design of GaAs-based radiation voltaic batteries is also beginning to be gradually realized for prototyping. By utilizing the high radiation absorption properties of GaAs, researchers have been able to create prototype batteries with high energy density. These prototype batteries are able to operate stably in high-radiation environments, providing a guaranteed power supply for long periods of time.

Future research will continue to focus on material innovation and structural design. In particular, with the advancement of nanotechnology and quantum dot technology, the electronic properties of GaAs can be better tuned to further improve the efficiency of radiation voltaic batteries. As the application fields of GaAs-based radiation voltaic batteries continue to expand, radiation protection and safety will become the focus of research. How to improve the radiation resistance of materials and ensure the safe use and storage of radioisotopes remains a key issue in the future development of the technology. As the demand for multifunctional integrated batteries increases, the integration of GaAs-based radiation voltaic batteries with other energy sources (e.g., solar cells, chemical batteries, etc.) may be investigated in the future to provide a more efficient, long-lasting, and reliable energy supply.

The research on GaAs-based radiation voltaic batteries has entered a more mature stage. From material optimization and performance enhancement to practical prototype development, GaAs radiation voltaic batteries have a promising future for aerospace, military, and extreme environment applications.

However, the commercialization process still faces a number of challenges, including cost, environmental protection, and safety. With technological advances, GaAs-based radiation voltaic batteries are expected to play a greater role in the future.

4 | Wide-Band Semiconductor-Based Radiation Voltaic Battery

4.1 | SiC-Based Radiation Voltaic Battery

SiC semiconductor material, as one of the earliest developed wide-bandgap semiconductor materials, has been applied to the field of radiation voltaic batteries relatively early. SiC has high radiation hardness, thermal conductivity, and carrier mobility. The bandgap of SiC is 3.2 eV (for ^{4}H-SiC), endowing it with excellent performance in high-temperature and high-radiation environments. Additionally, the low intrinsic carrier concentration and backscattering coefficient of SiC contribute to improve the ECE and output power of the battery.

Current research on SiC-based radiation voltaic batteries primarily focuses on optimizing device structures and improving electrode materials to enhance charge collection efficiency and ECE. Qian et al. [54] proposed a novel SiC P–I–N diode to reduce the limitations of material quality on ECE and further improve ECE. Based on an accurate SiC betavoltaic battery numerical model, they developed a SiC P–I–N diode with a thinned P-type region (TP), referred to as TP P–I–N, and a passivated layer surface field (PLSF), referred to as PLSF P–I–N, the conversion efficiency of SiC-based batteries has been significantly improved. Figure 6a–c shows cross-sections of these semiconductor conversion devices. Qiao et al. [26] optimized the fabrication process of SiC Schottky barrier diodes, designing a Schottky barrier diode with a circular geometry of 2000 μm in diameter, as shown in Figure 6d. Figure 6e presents its cross-sectional view. They successfully developed a betavoltaic battery based on 4H-SiC, achieving a conversion efficiency of over 2.8%. This battery demonstrated high stability and output power under irradiation from radioactive isotope sources. Furthermore, Li et al. [55] investigated a Ni Schottky betavoltaic battery based on 4H-SiC. They fabricated Schottky diodes using Ni as the Schottky metal on an n-type 4H-SiC substrate, as depicted in Figure 6f. Their findings revealed that optimizing electrode materials and device structures could significantly enhance the V_{OC} and J_{SC} of the battery. Experimental results showed that SiC-based batteries could effectively separate EHPs and generate stable output currents under irradiation from radioactive isotope sources.

In 2016, the then state-of-the-art betavoltaic batteries made by Widetronix [56] had achieved an ECE of 18.6% and an output power density of 157.73 nW cm^{-2} using a ^{4}H-SiC planar P–N junction diode and a $TiH^3{}_x$ foil. Although the 18.6% ECE is close to the theoretical limit, the output power density of 100 nW still falls short of the requirements for practical applications (e.g., MEMS devices require approximately 10 μW).

SiC batteries are in the near-practicalization stage due to their high radiation hardness and thermal stability and have been used in pilot applications in extreme environments such as

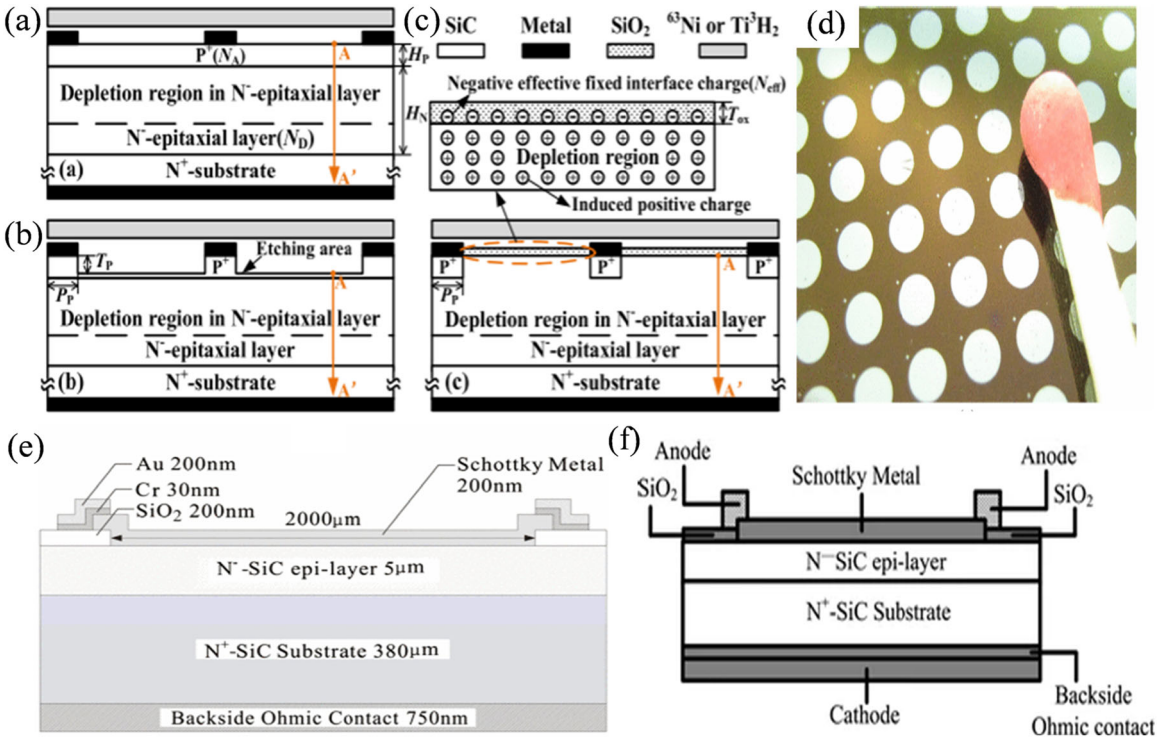

FIGURE 6 | (a) Cross-section of a P–I–N semiconductor conversion device. Reproduced with permission: Copyright 2022, IEEE [54]. (b) Cross-section of a TP P–I–N semiconductor conversion device. Reproduced with permission: Copyright 2022, IEEE [54]. (c) Cross-section of a PLSF P–I–N semiconductor conversion device. Reproduced with permission: Copyright 2022, IEEE [54]. (d) Circular structure of a Schottky diode. Reproduced with permission: Copyright 2011, IEEE [26]. (e) Cross-sectional view of a Schottky diode. Reproduced with permission: Copyright 2011, IEEE [26]. (f) Typical structure of a 4H-SiC Schottky diode. Reproduced with permission: Copyright 2010, Springer Nature [55].

nuclear reactor monitoring and deep space probes. Despite the remarkable progress in performance of SiC-based radiation voltaic batteries, they still face a number of challenges. First, how to further improve the conversion efficiency of the cells, especially the performance at low radioisotope activity, is the focus of current research. Second, the growth cost of SiC materials is high, how to reduce the preparation cost and promote its large-scale application is also an important direction for future research. The miniaturization and integration research of SiC-based batteries will provide a continuous and stable energy supply for modern microelectronic devices.

4.2 | GaN-Based Radiation Voltaic Battery

GaN, with a bandgap of 3.4 eV, is an even more attractive choice for manufacturing betavoltaic batteries. Moreover, GaN exhibits higher radiation resistance, making it suitable for operation under high-energy radioactive isotope sources such as ^{147}Pm and ^{90}Sr. Figure 7a illustrates the schematic of a GaN sensor PIN structure. The doping concentration of the GaN layer plays a critical role; lightly doped layers can achieve high-resistance (HR) GaN, resulting in a wider depletion region, increased EHP collection rates, and enhanced battery output. Metal-organic chemical vapor deposition (MOCVD) is currently the primary method for growing GaN. However, MOCVD-grown GaN faces challenges such as suboptimal crystal quality and difficulty in growing sufficiently thick HR GaN layers. Additionally, undoped GaN grown on sapphire substrates typically exhibits n-type conductivity (electron concentration $n > 5 \times 10^{16}\,\mathrm{cm}^{-3}$) due to residual impurities, while the hole concentration in MOCVD-grown p-type GaN is limited to around $1.5 \times 10^{17}\,\mathrm{cm}^{-3}$ [58, 59]. These limitations result in an excessively narrow depletion region in GaN P–N junction structures, hindering efficient collection of radiation-generated EHPs.

In 2011, Lu et al. [12] demonstrated that GaN Schottky diodes could be used as betavoltaic batteries. GaN films with a dislocation density of $1 \times 10^{8}\,\mathrm{cm}^{-2}$ were epitaxially grown via MOCVD. Through refined fabrication processes, they successfully produced GaN Schottky diodes with a reverse breakdown voltage exceeding 200 V, a Schottky barrier of 0.64 eV, and an ideal factor of 1.02. The GaN betavoltaic battery loaded with ^{63}Ni achieved the ECE and charge collection efficiency (CCE) of 0.32% and 29%, respectively, with V_{OC} and J_{SC} as low as 0.1 V and 1.2 nA cm^{-2}. The primary reason for the low output power was the thin effective active layer of the battery. Therefore, growing thick, high-resistance GaN films with low dislocation density became a key direction for improving battery performance. Later, Zai et al. [60] proposed a high open-circuit voltage betavoltaic battery based on a GaN P–I–N homojunction. The GaN epitaxial layer was grown on a 2-in. c-plane sapphire substrate using an MOCVD system. The low-electron-concentration n-type GaN layer was designed as the β-absorption layer, grown using a compensation doping process where Fe acceptor impurities were added to unintentionally doped GaN. Under irradiation from a solid ^{63}Ni source with an activity of 0.5 mCi, the betavoltaic battery with an effective area of $2 \times 2\,\mathrm{mm}^2$ achieved a maximum output

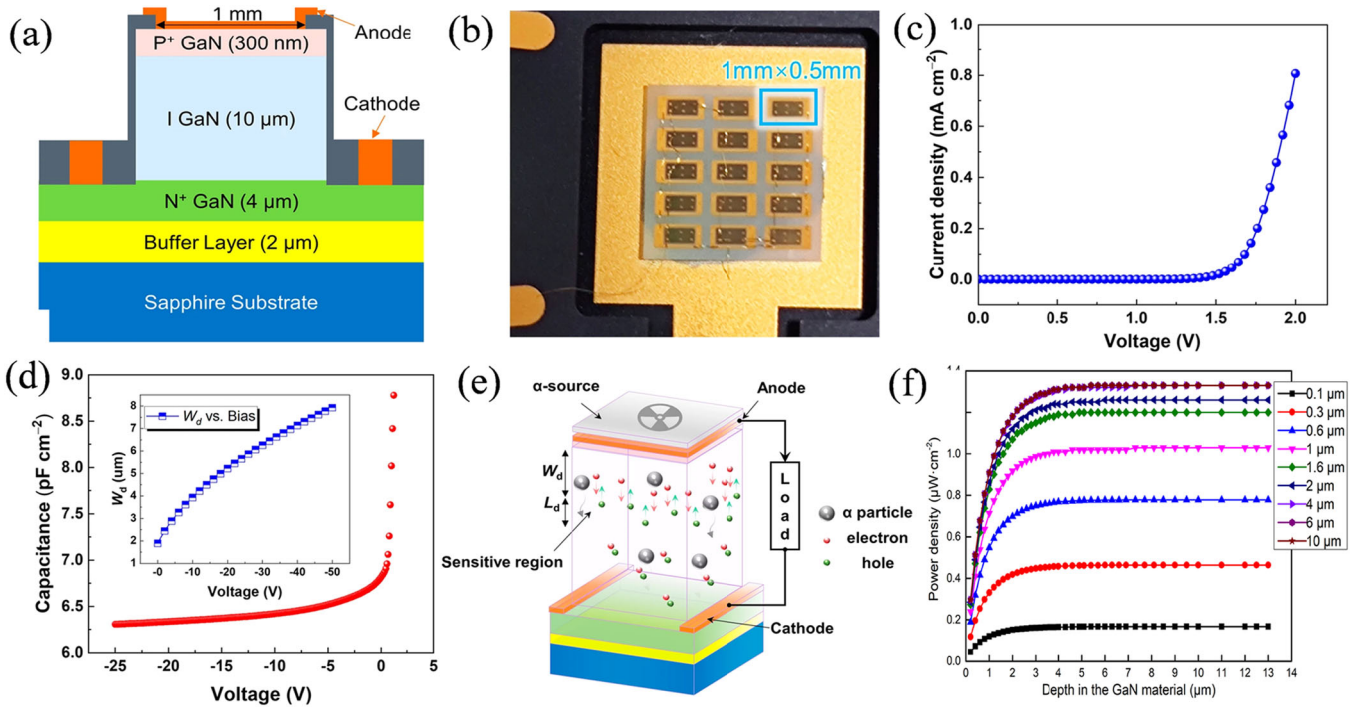

FIGURE 7 | (a) Typical structure of a GaN P–N junction betavoltaic batteries. Reproduced with permission: Copyright 2023, Springer Nature [15]. (b) Digital photo of the front view of a GaN sensor array. Reproduced with permission: Copyright 2023, Springer Nature [15]. (c) Forward *I–V* curve of a GaN sensor at room temperature without irradiation. Reproduced with permission: Copyright 2023, Springer Nature [15]. (d) Reverse *C–V* curve. Reproduced with permission: Copyright 2023, Springer Nature [15]. (e) Schematic of the interaction process between α particles and a GaN sensor. Reproduced with permission: Copyright 2023, Springer Nature [15]. (f) Relationship between energy deposition power density and radiation penetration depth in GaN material. Reproduced with permission: Copyright 2020, Elsevier [57].

power of 0.49 nW, $V_{OC} = 1.64$ V, $J_{SC} = 568$ pA. The maximum energy conversion efficiency, calculated as the ratio of maximum output power to radioactive isotope energy, was 0.98%.

In 2022, Toprak et al. [61] grew the epitaxial structure of a GaN-based betavoltaic battery via MOCVD and investigated p-type ohmic contacts with different Ni/Au metal thickness ratios, using temperature and N_2:O_2 (1:1) gas atmosphere, along with various surface treatments for this epitaxial structure. Transfer length method measurements were performed after each process condition to examine specific contact resistivity. GaN-based P–I–N betavoltaic batteries were fabricated and tested using a scanning electron microscope (SEM) as an electron source. Devices mounted on printed circuit boards (PCBs) were exposed to an electron current of 1.5 nA at 17 keV energy in the SEM. For a 1×1 mm^2 device, the dark current at 0 V was 2.8 pA, the fill factor was 0.35, the maximum power conversion efficiency was 3.92%, and the maximum output power was 1 μW. In 2023, Gao et al. [15] designed and studied an alphavoltaic battery based on a GaN sensor with a PIN structure. They found that isoelectronic aluminum doping was an effective method to improve the performance of GaN transducers by reducing unintentional doping concentration, deep trap concentration, and dislocation density in GaN epitaxial layers. The isoelectronic Al-doped battery exhibited a large depletion region of 1.89 μm at 0 V bias and a CCE of 61.6%, resulting in a high ECE of 4.51%, comparable to the best GaN betavoltaic batteries. Figure 7b shows a digital photo of the front view of a GaN sensor array, Figure 7c,d display the forward *I–V* and reverse *C–V* curves of the GaN sensor at room temperature without irradiation, Figure 7e illustrates the interaction process between α particles and the GaN sensor, and Figure 7f depicts the relationship between energy deposition power density and radiation penetration depth in GaN material [57]. This study advances the efficiency of alphavoltaic batteries, bridging the gap between isotope microbatteries and practical applications in extreme environments.

In NASA's "Millennium Challenge" program, GaN is listed as a key material for radiation-resistant electronics, which may be used to power the Moon/Mars base in the future. However, most of the current research is in the prototype verification stage. The main bottleneck is the insufficient thickness of MOCVD-grown high-resistance GaN layers, resulting in a thin effective active layer and high dislocation density, which affects carrier collection. Optimization requires breakthroughs in thick-layer GaN epitaxy technology (e.g., hydride vapor phase epitaxy HVPE) and compensated doping processes. Multiple experimental results demonstrate that the wide-bandgap semiconductor GaN is a highly promising candidate for long-life radiation voltaic batteries.

4.3 | Titanium Dioxide-Based Radiation Voltaic Battery

Titanium dioxide (TiO_2)-based radiation voltaic battery is a kind of isotope battery utilizing TiO_2 as a semiconductor material. TiO_2 is a widely used wide-band semiconductor material with high stability, low cost, and good electronic and optical properties. Although the application of TiO_2 in radiation voltaic batteries started late, it has gradually attracted academic attention in terms of radiative energy conversion and battery performance.

TiO_2 has a broad forbidden band of about 3.0 eV and excellent chemical stability, especially in radiation environments, where it can withstand the impact of energetic particles without structural degradation. This characteristic makes it particularly important for applications in extreme environments. Compared with other high-performance semiconductors (e.g., GaAs, SiC, etc.), TiO_2 material is abundantly available and inexpensive, and it also excels in the photoelectric effect [62], which provides an additional advantage in radiation voltaic batteries, and thus has the potential to be a cost-effective material for isotope batteries.

The radiative voltaic effect of TiO_2 as a semiconductor material began to receive attention in studies conducted between the late 1990s and early 2000s. At that time, research focused on the radiative response properties of TiO_2, and experiments showed that TiO_2 could effectively convert radiant energy into electrical energy. In early experiments, researchers found that TiO_2 was able to generate a stable electric current under the excitation of high-energy particles, proving that it has some ability to convert radiant energy [63, 64]. However, due to the poor electrical conductivity of TiO_2, its initial radiation voltaic batteries output power is low. In 2014, Kwon's group [65] reported a radiation voltaic battery of Pt/nano-porous TiO_2 for effective energy conversion of radioisotopes as shown in Figure 8a. The report pointed out that the poor electrical conductivity of the pristine TiO_2NTAs was unfavorable to the charge-carrier transport. which can lead to rapid complexation of the EHPs.

To solve the problem of poor electrical conductivity of TiO_2, researchers have started to modify TiO_2 by nanosizing techniques. For example, TiO_2 was made into nanoparticles, nanotubes, nanowires, and other forms to increase its surface area and improve the electron mobility. It has been found that nanosized TiO_2 has higher radiation energy conversion efficiency. In 2018, Wang et al. [66] reported a defect-induced betavoltaic cell, as shown in Figure 8b, where TiO_2NTAs prepared by electrochemical anodic oxidation and argon (Ar) annealing techniques were used as β-radiation absorbing materials, and a ^{63}Ni source (20 mCi) was sandwiched between TiO_2NTAs and Ni substrate to enhance the performance. The samples were heat-treated at 650°C and 450°C in Ar and air environments. The Ar-annealed samples at 650°C showed excellent performance compared to the air environment, with ECE, V_{OC}, J_{SC}, and maximum power density of 3.65%, 1.13 V, 103.3 nA cm^{-2}, and 37 nW cm^{-2}, respectively. Chen et al. fabricated arrays of TiO_2NTAs as well as electrochemically reduced graphene oxide (G-TNTA) and a ^{63}Ni source (10 mCi) constituting a sandwich-type betavoltaic cell (Ni/^{63}Ni/G-TNTAs/Ti) with an ECE of 3.93%, V_{OC} of 2.38 V, and J_{SC} of 14.69 nA cm^{-2}. In 2018, Ma et al. [67] prepared Schottky junction radiation voltaic batteries using TiO_2NTAs, as shown in Figure 8c, and the V_{OC} of the device was obtained to be 1.04 V, the FF was 0.32, and the maximal output power was 39 mW cm^{-2} by using a 20 mCi ^{63}Ni isotope source test.

To improve the electrical conductivity and radiation response efficiency of TiO_2 materials, researchers have also [68, 69]

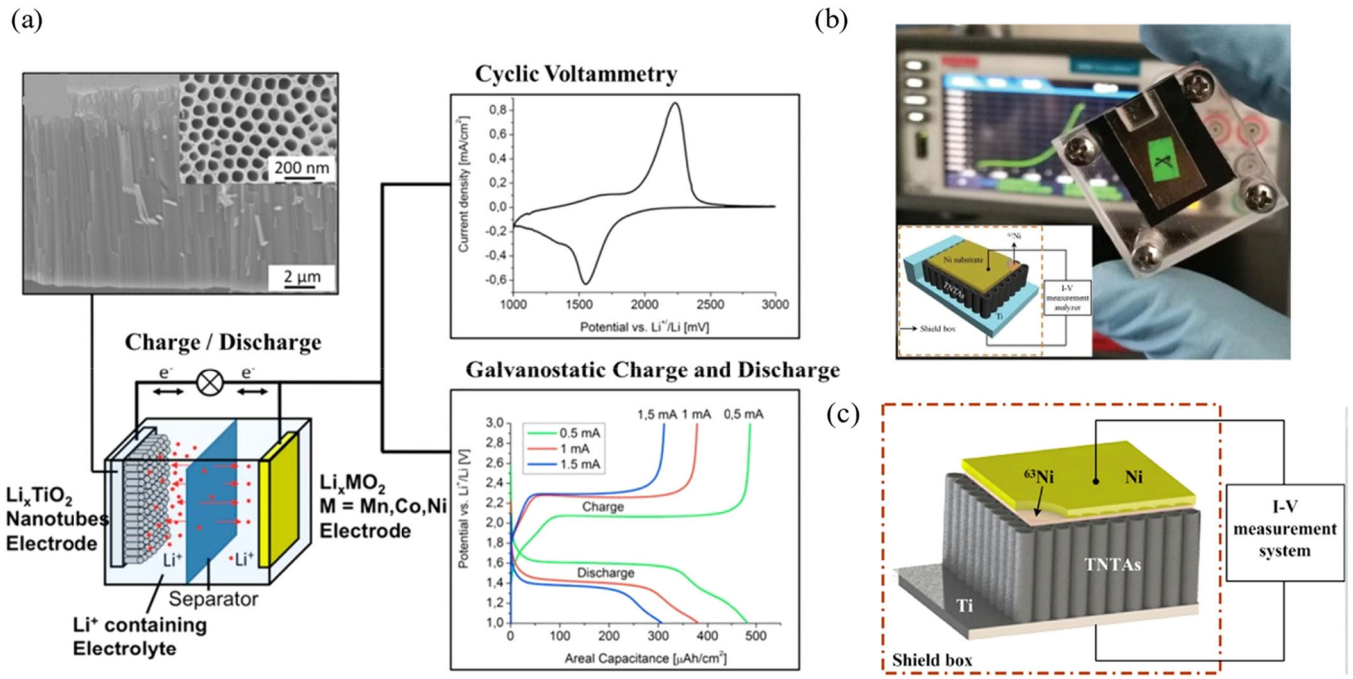

FIGURE 8 | (a) A Pt/nanoporous TiO_2 radiolytic cell for effective energy conversion of radioisotopes reported by Kwon's group. Reproduced with permission: Copyright 2014, American Chemical Society [65]. (b) A defect-induced betavoltaic cell reported by Wang et al. Reproduced with permission: Copyright 2018, RSC Pub [66]. (c) Titanium dioxide nanotube array Schottky junction radiation voltaic batteries. Reproduced with permission: Copyright 2018, American Chemical Society [67].

tried to improve the electronic properties of TiO_2 by doping with other elements. The doped TiO_2 materials were able to respond better to radiation and increase the efficiency of converting radiant energy into electrical energy. Li et al. [70] prepared Ag, copper (Cu) co-doped TiO_2 by sol-gel method, and found that the half-height broadening of the diffraction peaks at the (101) crystal plane of TiO_2 appeared after co-doping suggesting that the doping of Ag, Cu induced the lattice distortion in anatase structure, and from the point of view of grain size Cu, Ag co-doping inhibited the enlargement of anatase TiO_2 grains, and smaller anatase TiO_2 was obtained, but Cu, Ag co-doping did not cause changes in TiO_2 morphology. The energy band gap of Ag, Cu co-doped samples mostly ranged from 1.87 to 2.40 eV, suggesting that after Ag, Cu co-doping, the energy band structure of TiO_2 changed, and electrons were more prone to jumping.

TiO_2 not only exhibits better energy conversion ability in radiation environment but also its own photoelectric effect under light makes its potential for application in radiation voltaic batteries further increase. Researchers have explored the utilization of the combined photovoltaic and radiative volt effect of TiO_2 to further increase the energy output. The performance of TiO_2-based radiation voltaic batteries in high-radiation environments has been gradually verified. Experimental results show that the TiO_2 material can maintain high stability under long-term high-radiation conditions, and its current output has strong continuity.

In the 2020s, prototypes of TiO_2-based radiation voltaic batteries began to be put into practical applications and experiments. By optimizing the structure, doping, and matching of TiO_2 with the radiation source, it presents its excellent radiation response performance and low cost, and gradually shows its potential in deep space exploration and space applications. In the short term, the application of TiO_2-based radiation voltaic batteries will focus on special fields; the current research idea is to combine diamond, SiC and other high-radiation-resistant materials to improve the power density and lifetime, and to explore the 3D trench structure or liquid-mediated energy capture mechanism to optimize the carrier collection efficiency. Compared with traditional chemical batteries or solar cells, TiO_2-based radiation voltaic batteries have irreplaceable advantages in space environments far from the sun and with high radiation.

4.4 | ZnO-Based Radiation Voltaic Battery

ZnO has a direct bandgap of 3.37 eV and is part of the third-generation semiconductors, alongside SiC and GaN. ZnO and GaN share similar bandgaps, densities, and electron densities. However, ZnO has a higher bandgap/exciton binding energy ($E_g/E_{e\text{-}h}$) ratio compared to GaN, which means it can generate more EHPs and achieve higher efficiency under the beta voltaic effect. ZnO films exhibit high transparency and conductivity and can be grown as single-crystal substrates at room temperature, making them promising materials for optoelectronic applications, high-speed devices, and space technology.

Ding et al. [71] proposed the use of hydrothermal synthesis to grow ZnO nanorod arrays (ZNRAs) for ^{63}Ni-powered betavoltaic cell. Based on experimental measurement data, a quantitative model was established to simulate the dark

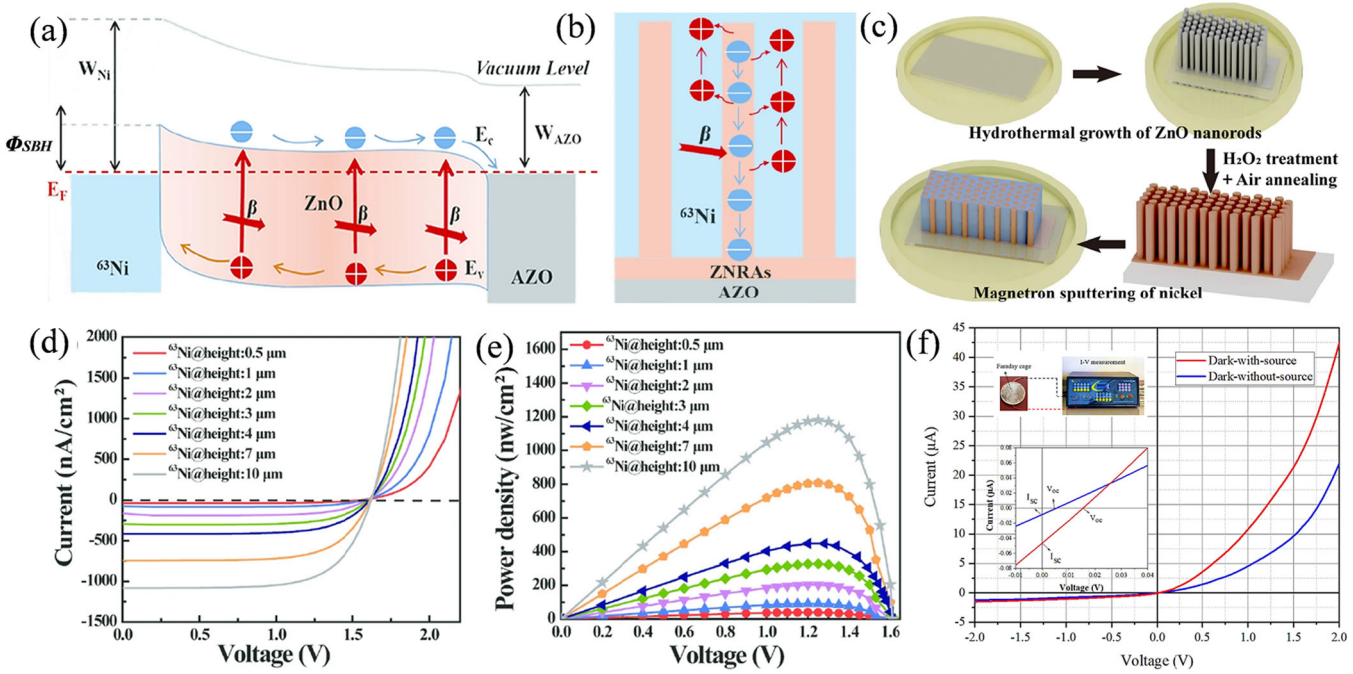

FIGURE 9 | (a) Schematic energy band diagram of betavoltaic cell based on ^{63}Ni ZNRAs. Reproduced with permission: Copyright 2022, Springer Nature [71]. (b) Transferring process of β-excited carriers in ^{63}Ni@ZNRAs. Reproduced with permission: Copyright 2022, Springer Nature [71]. (c) Schematic illustration of preparation process flow of Ni-incorporated ZNRAs structure. Reproduced with permission: Copyright 2022, Springer Nature [71]. (d) *I–V* and (e) *P–V* characteristics of devices based on ^{63}Ni@ZNRAs with different nanorod spacings. Reproduced with permission: Copyright 2022, Springer Nature [71]. (f) *I–V* properties of the fabricated device before and after radiation in the dark conditions (in Faraday cage). Reproduced with permission: Copyright 2025, Elsevier [72].

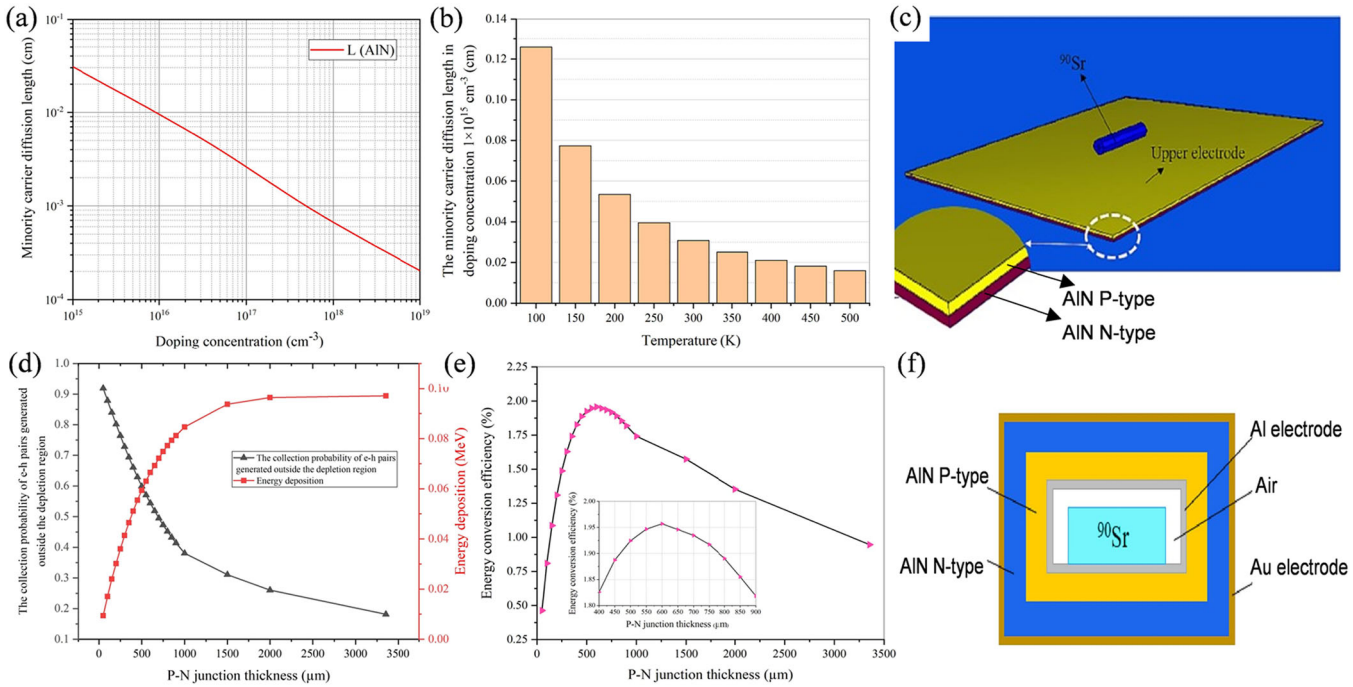

FIGURE 10 | (a) Minority carrier diffusion length as a function of doping concentration in AlN at 300 K. Reproduced with permission: Copyright 2023, Elsevier [74]. (b) Minority carrier diffusion length versus temperature at a doping concentration of 1×10^{15} cm^{-3}. Reproduced with permission: Copyright 2023, Elsevier [74]. (c) MCNP simulation model (Model 1) for the AlN-^{90}Sr betavoltaic cell. Reproduced with permission: Copyright 2023, Elsevier [74]. (d) Plot of the amount of energy deposited in the P–N junction and the probability of collecting EHPs generated outside the depletion region, versus different thicknesses of AlN P–N junction. Reproduced with permission: Copyright 2023, Elsevier [74]. (e) Battery efficiency versus AlN P–N junction thickness variation. (f) MCNP simulation model (Model 3) for the AlN-^{90}Sr betavoltaic cell. Reproduced with permission: Copyright 2023, Elsevier [74].

characteristic parameter values of simulated betavoltaic cell based on Ni-doped ZNRAs structures. Through MCNP simulations, numerical values for the β-particle deposition energy in ZNRAs were obtained under different nanorod spacings and heights. By simulating and optimizing 3D ZNRAs and 2D ZnO bulk structures, the performance of ^{63}Ni-powered betavoltaic cell based on these two structures was evaluated using the quantitative model. Betavoltaic cell based on 3D ZNRAs and 2D ZnO bulk structures achieved maximum ECE values of 10.1% and 4.69%, respectively, indicating that 3D nanostructured wide-bandgap semiconductors have a significant advantage in enhancing the ECE of betavoltaic cells. Figure 9a shows the band structure diagram of a betavoltaic cell based on a ^{63}Ni ZnO nanorod array; Figure 9b illustrates the transfer process of β-excited carriers in the ^{63}Ni ZnO nanorod array. Figure 9c shows the schematic diagram of the preparation process for the Ni-doped ZnO nanorod array structure. Figure 9d,e presents the *I–V* and *P–V* curves measured for ^{63}Ni ZNRAs devices with different nanorod spacings.

Movahedian et al. [72] fabricated an n-Si/ZnO heterojunction using the chemical bath deposition (CBD) technique to place ZnO nanospheres on an n-Si (100) substrate. Aluminum (Al) and gold (Au) electrodes were deposited on the sample, which was then exposed to an external ^{90}Sr/^{90}Y radiation source with an activity of 12.8 mCi. The *I–V* characteristics of the devices manufactured before and after radiation (Faraday cage) measured under dark conditions are shown in Figure f. The J_{SC}, V_{OC}, ECE, and maximum output power were measured as 0.047 μA, 0.015 V, 3.4×10^{-4}%, and 0.141 nW, respectively. Later, Maghsodi et al. [73] conducted a novel study on betavoltaic cells with a non-flat design, focusing on a Schottky structure combining ZnO as the semiconductor with a ^{90}Sr/^{90}Y radiation source. They achieved a converter with a solid cylindrical power source and a flat geometry. The results demonstrated that optimizing the geometric configuration could significantly enhance the performance of betavoltaic cells.

ZnO is theoretically suitable for micro-energy supply for flexible electronics and wearable devices due to its high exciton binding energy and low-cost deposition process. However, existing experiments are extremely inefficient and can only drive picowatt-scale loads. Maturity is currently at an early stage in the lab.

Other wide-bandgap semiconductor materials include AlN and InN, but research on them is limited. For example, Movahedian et al. [74] studied an AlN betavoltaic cell driven by a ^{90}Sr/^{90}Y radioactive isotope source. Using MCNP simulations, they investigated the effects of electrode type, size, thickness, and P-N junction geometry on battery efficiency. Figure 10a shows the minority carrier diffusion length as a function of doping concentration in AlN at 300 K, while Figure 10b illustrates the relationship between minority carrier diffusion length and temperature at a doping concentration of 1×10^{15} cm^{-3}. Figure 10c shows the AlN-90Sr betavoltaic cell model 1 in the MCNP simulation setup. Compared to AlN P–N junctions of different thicknesses, the energy deposited in the P–N junction and the probability of ehpS generated outside the depletion region are shown in Figure 10d. The relationship between battery efficiency and the thickness of the AlN P–N junction is shown in Figure 10e. Finally, it was found that the cubic model has the highest J_{SC}, V_{OC}, and ECE, which are 406.05 nA, 5.43 V, and 5.16%, respectively. To compare the efficiency of the AlN betavoltaic cell with that of GaN and SiC betavoltaic cell, model 3 (Figure 10f) was studied based on the optimal dimensions obtained for GaN and SiC in model 1. Simulation results indicate that the efficiency of the AlN betavoltaic cell is 24% higher than that of the GaN betavoltaic cell and 975% higher than that of the SiC betavoltaic cell. It can thus be seen that AlN is also a very promising semiconductor material. Future research can focus on exploring these emerging semiconductor materials to optimize battery performance.

5 | Ultra-Wide Bandgap Semiconductor-Based Radiation Voltaic Battery

5.1 | Diamond-Based Radiation Voltaic Battery

Diamond is an ideal material for constructing the junction components of radiation voltaic isotope batteries due to its wide bandgap (5.5 eV), excellent thermal conductivity, carrier mobility, and radiation resistance. Since energy conversion units are continuously exposed to high-energy particle irradiation, degradation effects caused by radiation-induced damage are critical factors in the design and fabrication of such devices. Radiation-resistant materials can significantly extend battery lifespan. Moreover, diamond's high radiation tolerance allows the use of radioactive isotopes emitting higher-energy particles as power sources. Higher incident particle energies enable greater electrical power generation within a given battery volume, making diamond-based conversion devices highly promising for enhancing the output power of nuclear microbatteries.

In 2015, Bormashov [17] tested a prototype nuclear microbattery with a total effective area of approximately 15 cm^2 and characterized its performance under different types of radioactive isotope sources. The electron beam-induced current (EBIC) technique in SEM was used to study the energy conversion efficiency of the fabricated diamond Schottky diodes. Each of the 130 Schottky barrier diamond diodes achieved a typical ECE of about 5%. Liu et al. [75] fabricated a diamond Schottky energy conversion device with a high-quality intrinsic layer, as shown in Figure 11a. Using this structure, they obtained a V_{OC} of 1.06 V and an ECE of 1.41%. Figure 11b shows the dark current curve of the diode, and Figure 11c presents the alpha voltaic performance under different ^{241}Am source activities. To further improve the open-circuit voltage, Liu et al. [76] inserted a ~10-nm-thick ZnO layer as an electron transport layer between the Schottky electrode and the diamond intrinsic layer. Figure 11d displays the Raman spectrum of the diamond intrinsic layer, while Figure 11e, f illustrate the band diagrams of the devices without and with the ZnO layer, respectively. The reduction in carrier collection efficiency caused by hole diffusion to the metal electrode from the intrinsic layer could be

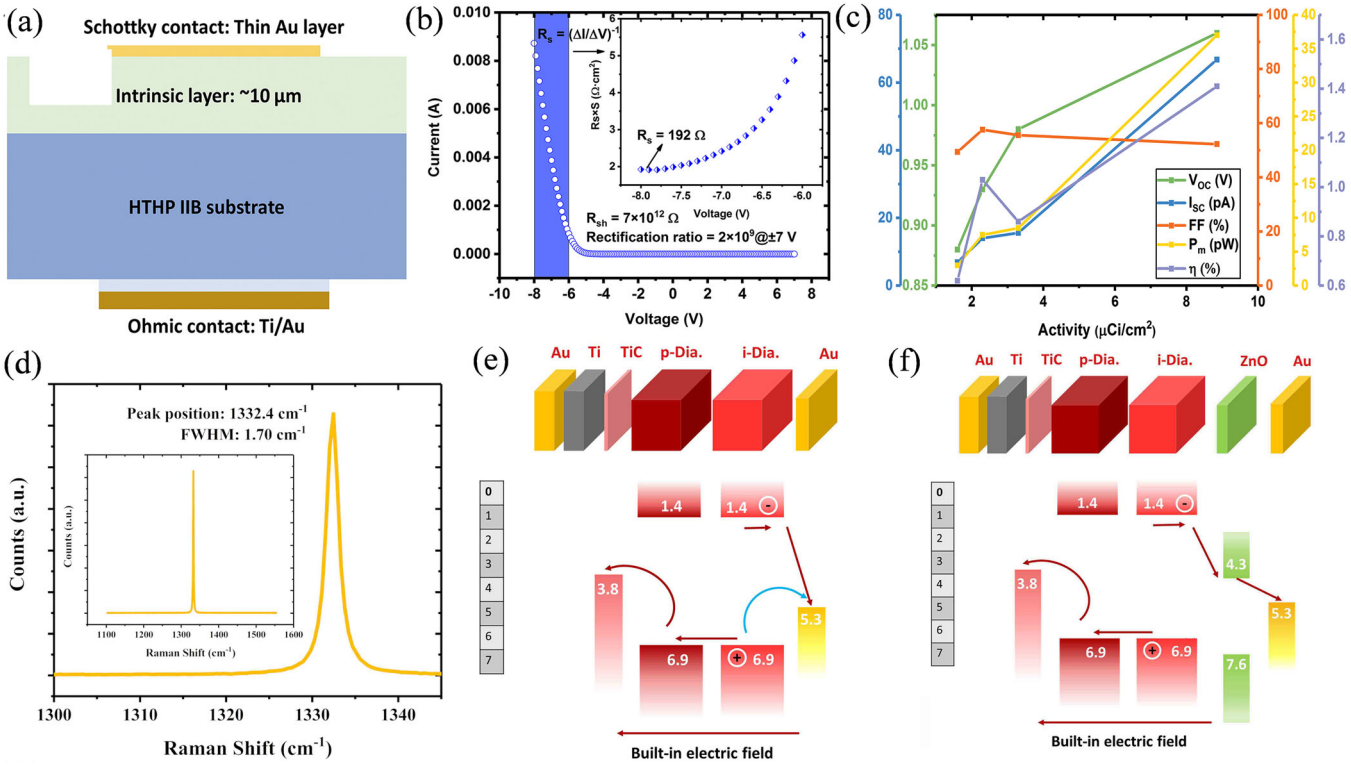

FIGURE 11 | (a) Schematic of the diamond Schottky barrier energy converter. Reproduced with permission: Copyright 2019, John Wiley and Sons [75]. (b) Dark current curve of the diode. Reproduced with permission: Copyright 2019, John Wiley and Sons [75]. (c) Alpha volt performance at different ^{241}Am activity sources. Reproduced with permission: Copyright 2019, John Wiley and Sons [75]. (d) Raman spectrum of the diamond intrinsic layer. Inset: Raman spectrum over a larger wavenumber range. Reproduced with permission: Copyright 2020, Elsevier [76]. (e) Band diagram of the device without the ZnO layer (f) Band diagram of the device with the ZnO layer. Reproduced with permission: Copyright 2020, Elsevier [76].

effectively blocked by the oxide layer. The high potential of the ZnO layer on the intrinsic layer was effectively characterized using Kelvin force microscopy. This visual demonstration successfully shows the mechanism of V_{OC} gain, culminating in the realization of a Schottky isotope single component with an impressive V_{OC} of up to 1.43 V. These data have important implications for Schottky isotope batteries.

However, the current diamond-based radiation voltaic isotope battery is still in the laboratory exploration stage, the challenge lies in the high cost of large-area high-quality diamond growth and the need to break through the diamond doping technology. Overall, there is considerable room for process optimization.

5.2 | β-Ga_2O_3-Based Radiation Voltaic Battery

The research process of gallium oxide (β-Ga_2O_3)-based radiation voltaic battery has received much attention in recent years. Gallium oxide is a semiconductor material with an extremely wide forbidden band, and its excellent electrical, optical, and chemical properties make it potentially applicable in several fields, especially in radiation voltaic batteries. Although the current preparation process is not yet mature enough to produce stable crystalline structures, β-Ga_2O_3 gallium oxide is one of the ideal materials for radiation energy conversion due to its stability in high-radiation environments, excellent electronic conductivity, and high-temperature resistance [77–79].

The band gap of gallium oxide is about 4.8 eV, which is much higher than that of traditional semiconductor materials such as Si and GaAs. This means that β-Ga_2O_3 materials have excellent stability under high radiation conditions and can withstand the impact of energetic radiation particles without significant performance degradation [80]. In particular, β-Ga_2O_3 demonstrates good tolerance for the radiation response of α-particles, β-particles, and γ-rays. It also has high carrier mobility and electronic conductivity, which enables it to efficiently convert radiation energy into electrical energy [81].

The study of β-Ga_2O_3-based radiation voltaic batteries started late, but with the development of materials science and semiconductor physics, β-Ga_2O_3 began to attract the attention of scholars. Early research focused on the material properties of β-Ga_2O_3, especially its stability in high-energy radiation environments [82, 83]. Experiments have shown that β-Ga_2O_3 materials can respond to external radiation and generate electric current. Researchers have begun to explore the use of this property of β-Ga_2O_3 to develop radiation voltaic batteries based on this material.

The preparation techniques and crystal growth methods of gallium oxide were continuously improved. Researchers have improved the radiation response and current output capabilities of β-Ga_2O_3 by adjusting its crystal structure, doping elements, and surface treatment. For example, doping elements such as nitrogen (N) or boron (B) have been used to improve the conductivity and stability of gallium oxide,

thereby optimizing its performance in a radiation environment. Experiments have shown that doping β-Ga_2O_3 can effectively enhance its voltage output and current response in a radiation environment. The responsiveness of β-Ga_2O_3 to high-energy radiation particles was significantly improved, exhibiting high ECE [84]

A distinctive feature of gallium oxide-based radiation voltaic batteries is their long lifetime and high stability. In experiments, β-Ga_2O_3-based radiation voltaic batteries are able to stabilize the output current in a prolonged radiation environment and exhibit a very long operating life, which makes them have great potential for application in deep space exploration and long-term radiation monitoring. Compared with traditional semiconductor materials such as Si and GaAs, β-Ga_2O_3 performs better in terms of radiation energy conversion efficiency and radiation resistance. Therefore, β-Ga_2O_3-based radiation voltaic batteries may gradually replace conventional materials in the future radiation voltaic batteries field, especially for applications in high radiation environments [85].

Although β-Ga_2O_3-based radiative radiation voltaic batteries show great potential in theory and experiment, their commercial application still faces some challenges: the production cost of β-Ga_2O_3 is relatively high, especially in the synthesis of high-purity, high-quality gallium oxide materials, which still requires a lot of research and process improvement. How to reduce the production cost of gallium oxide materials and achieve scale production is one of the main challenges at present.β-Ga_2O_3-based radiation voltaic battery is an important research direction in the field of nuclear batteries at present. With its excellent radiation tolerance, wide bandgap and high-temperature stability, β-Ga_2O_3-based radiation voltaic batteries show great potential for applications in deep space exploration, nuclear energy monitoring, and military security. Although there are still some technical challenges, and still exists in the theoretical stage, but with the β-Ga_2O_3 materials research continues to deepen and the related technology progress, β-Ga_2O_3-based radiation voltaic battery is expected to become an important radiation energy conversion material in the future.

6 | Novel Material-Based Radioisotope Battery

6.1 | Perovskite-Based Radioisotope Battery

Perovskite material-based radioisotope batteries have attracted much attention in recent years as an emerging material for nuclear energy conversion. Perovskite materials have become a research hotspot due to their excellent performance in the fields of photovoltaics and thermoelectricity, especially in solar cells. Meanwhile, the application of perovskite materials in radioisotope batteries has also been gradually emphasized.

Perovskite materials usually referred to as crystal-structured materials with the chemical formula ABX_3, where A is an organic or inorganic cation (e.g., MA^+, FA^+, Cs^+), B is a metal cation (e.g., Pb^{2+}, Sn^{2+}), and X is a halogen anion (e.g., Br^-, I^-), and such a structure provides a rich chemical composition and a good crystalline integrity. The excellent optical and electrical properties, good radiation responsiveness, and good structural tunability make them one of the ideal candidates for the study of radioisotope batteries. Perovskite materials have the following important physicochemical properties, which make them show great potential in radioisotope batteries: Perovskite materials usually have a wide bandgap and high light absorption coefficients, which makes them excellent in the field of photoelectricity conversion, and are able to efficiently absorb the energy from external sources of radiation and convert it into electrical energy. Perovskite materials have high carrier mobility and can effectively transport electrons and holes generated by radiation, thus improving the ECE of the battery.

Certain perovskite materials (e.g., lead perovskite, perovskite oxides, etc.) have a wide bandgap and are able to withstand higher energy radiation without significant loss of electrons, and therefore have better radiation tolerance and are suitable for use in the conversion of electrical energy in a radiation environment. The structure of perovskite materials can be optimized by doping, adjusting the composition, and regulating the crystal structure to achieve higher ECE in different radiation environments [86].

Early studies focused on the performance of perovskite materials under high-energy radiation. It has been shown that perovskite materials are able to effectively convert radiant energy into electrical energy under high-energy particle radiation, and their response is especially excellent under microwave, ultraviolet, and radiant particle impacts. In 2017, Chen et al. first verified the radioisotope photovoltaic effect of fully inorganic perovskite quantum dots $CsPbBr_3$ in different solvents as well as different X-ray irradiation environments [87], and analyzed its mechanism. It is concluded that the fully inorganic perovskite quantum dot $CsPbBr_3$ is a novel fluorescent material with tunable emission spectra and can be applied to radioisotope photovoltaic battery. In 2018, C. Wang et al. prepared $CsPbBr_3$ and $CsPbBr_{1.5}I_{1.5}$ perovskite quantum dots (QDs) for use in radioisotope photovoltaic batteries using a thermal injection method. The results showed that the system exhibited both radioluminescence and photoluminescence effects, the addition of QDs improved the optical and electrical properties of the cell, and the perovskite quantum dots showed great potential in radioisotope photovoltaic batteries and X-ray imaging technology [88]. In 2019, Xu et al. analyzed the performance of $CsPbBr_3$ quantum dot thin films as transducer materials in radioisotope photovoltaic batteries, which concluded that $CsPbBr_3$ perovskite quantum dot films can be used as an energy conversion layer for radioluminescence [89].

The stability of perovskite materials in high-temperature, high-radiation environments has gradually become a key research direction. Perovskite materials degrade under high temperatures or long-term radiation environments, so improving the long-term stability and durability of these materials has become an important area of research (Figure 12).

After entering 2020, the research on perovskite material-based radioisotope photovoltaic batteries began to enter the practical

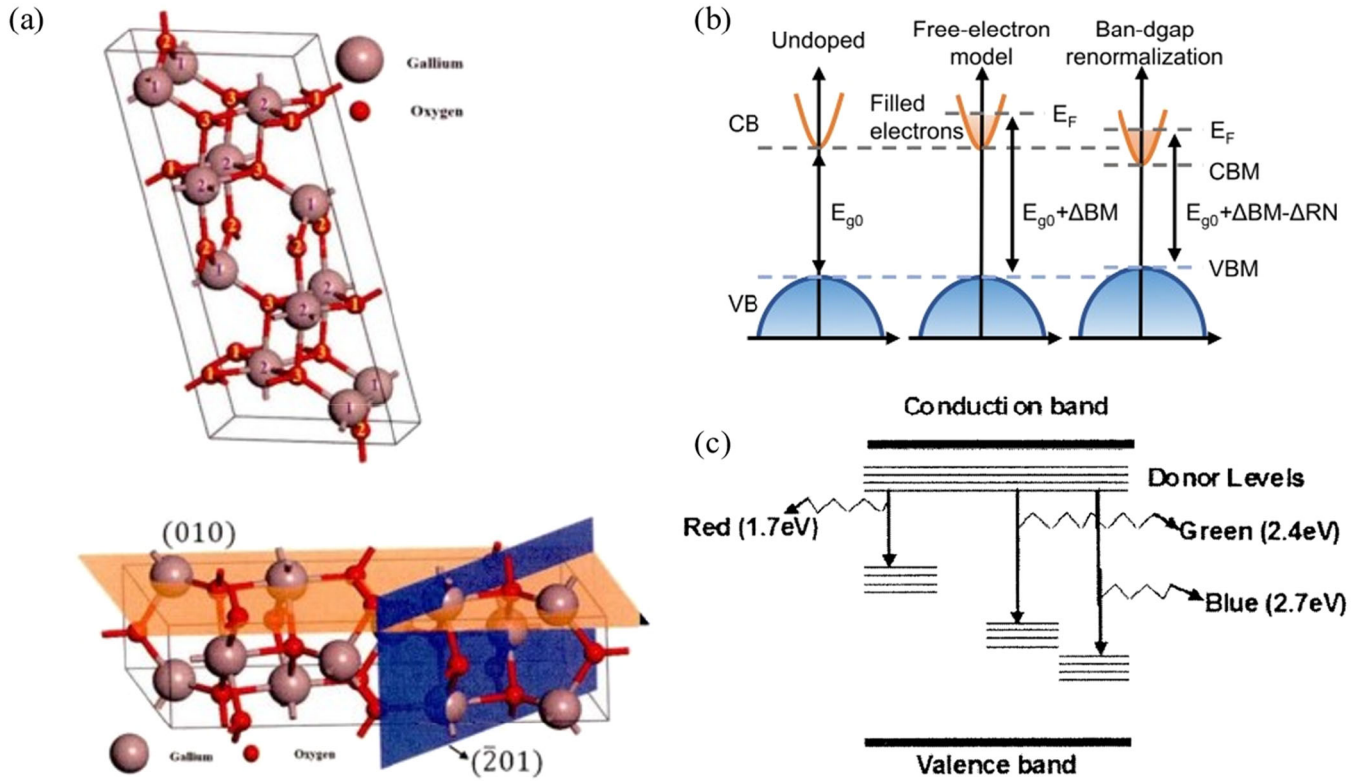

FIGURE 12 | (a) β-Ga_2O_3 crystal structure. Reproduced with permission: Copyright 2018, AIP Publishing [17]. (b) Schematic of the electronic structure change of Si-doped Ga_2O_3. Reproduced with permission: Copyright 2022, American Physical Society [84]. (c) Luminescence mechanism of β-Ga_2O_3 nanorods. Reproduced with permission: Copyright 2016, AIP Publishing [81].

application stage, and in 2021, Xu et al. studied the application of $CsPbBr_3$ perovskite quantum dots in radioisotope photovoltaic batteries and showed that $CsPbBr_3$ perovskite quantum dots thin-film materials could improve the electrical performance of the battery [90]. Recently, Li et al. published a $Cs_{0.05}MA_{0.1}FA_{0.85}PbI_3$ perovskite (MA refers to methylammonium, FA refers to methylamine) photovoltaic core battery, which achieved a total power conversion efficiency of 0.889% and a continuous stable operating time of 1 year. The stability of perovskite-based radioisotope photovoltaic batteries under α-particle flow irradiation conditions and the superiority of perovskite materials as EHP separation/transport materials in radioisotope photovoltaic batteries were demonstrated [91]. And since the energy of β-particles is usually lower than that of α-particles (mostly in the range of 0.1–1 MeV), it can be assumed that the irradiation resistance of perovskite materials can fully satisfy the requirements of the special working environment of β-source radioisotope photovoltaic batteries. While Li et al. simulated the β radiation source by the electron gun of KYKY-EM6200 SEM, the $MAPbBr_3$ perovskite material achieved a conversion efficiency of 5.35% in the irradiation of high-energy electron beam (accelerating voltage of 15 kV) generated by the electron gun, as shown in Figure 13a [19], which proves the resistance of the perovskite material to β-radiation.

Second, perovskite materials are more tolerant to point defects, which allows them to maintain good electrical properties in radiation environments [93, 94]. Even with the presence of a large number of point defects, their carrier diffusion length can still reach several hundred nanometers, which is much higher than that of conventional polysilicon materials. This is because two mechanisms exist in perovskite materials to mitigate irradiation damage. First, the presence of heavy elements such as lead in the material enhances the blocking ability of high-speed particle streams and reduces the penetration damage of incident particles into the deeper layers of the material. As shown by Gao et al. in Figure 13b, FACs perovskite can still maintain much higher ECE than that of Si-based nuclear cells after irradiation with He ion beam [20]. Second, special structures such as quantum dots and nanowires can reduce the defect state density of perovskite materials by means of surface passivation while increasing their carrier collection paths. Tang et al. achieved effective protection against 200 KeV H+ ionic currents based on $CsPbBr_3$ quantum dots prepared by the thermal injection method [89]; similarly, Chen et al. combined $MAPbBr_3$ quantum dots with PPO (2,5-diphenyl oxazole) composite to develop a novel photovoltaic nuclear cell with a sixfold improvement in ECE over the silicon-based core cell system [88]. This part of the research uses fluorescent materials to convert "beta rays → visible light (fluorescence) → electrical energy," thereby achieving high ECE [87–89], indirectly proving the tolerance of perovskite materials in irradiation environments and their applicability in radioisotope batteries.

In addition, perovskite photovoltaic cells have been shown to recover or heal after radiation damage. Its special self-healing ability can repair lattice defects caused by radiation to some extent [25]. This self-healing ability, which originates from the soft lattice characteristics and ion migration mechanism of perovskite, can promote postirradiation repair at specific

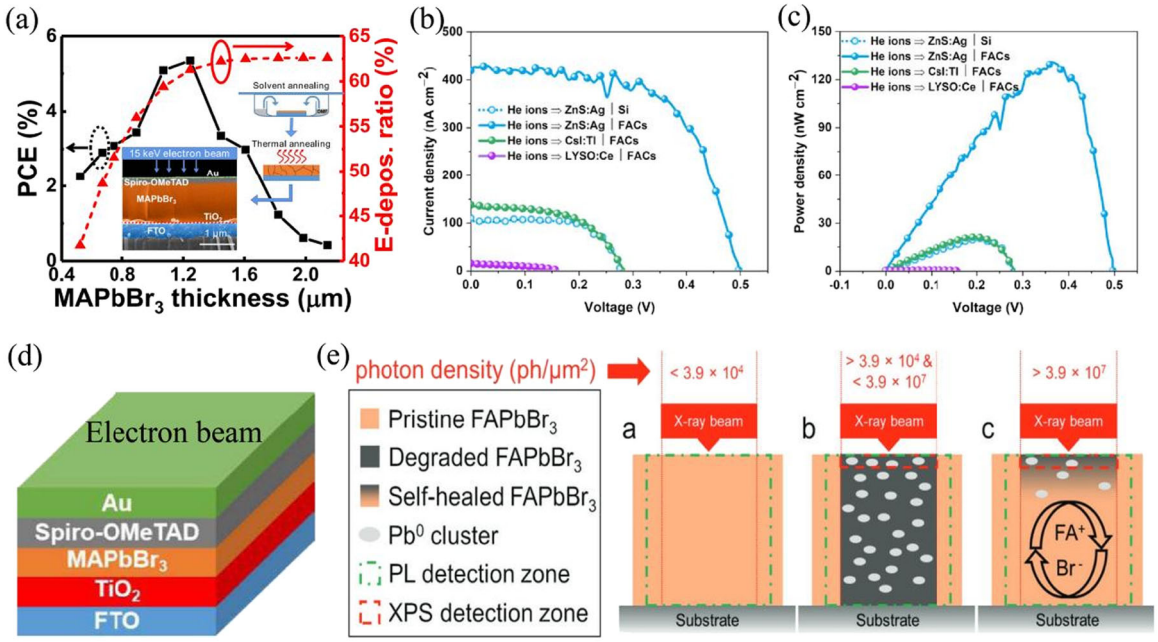

FIGURE 13 | (a) Energy conversion rate, energy deposition rate versus material thickness of $MAPbBr_3$-based β-source radioisotope cells. Reproduced with permission: Copyright 2021, American Chemical Society [19]. (b) *J–V* curve and (c) *P–V* curve of perovskite-based radioisotope photovoltaic batteries and Si-based radiation voltaic batteries under He ion irradiation. Reproduced with permission: Copyright 2022, John Wiley and Sons [20]. (d) Schematic diagram of the device structure of the $MAPbBr_3$-based β-source radioisotope cells. Reproduced with permission: Copyright 2021, American Chemical Society [19]. (e) Schematic diagram of the degradation/self-healing process of $FAPbBr_3$ under x-rays. Reproduced with permission: Copyright 2023, John Wiley and Sons [92].

energies, thereby maintaining battery performance. For example, the lattice structure of methylammonium lead iodide can be spontaneously restored at room temperature after neutron irradiation [95], and the restoration process is usually completed in a few hours to a few days; while lead bromide cesium ammonium has been shown to show a "drop-off-recovery" dynamics in its photovoltaic performance after irradiation with high doses of X-rays, as shown in Figure 13e, which shows that perovskite can be self-healed by its soft lattice properties and ion mobility mechanism. Again, the self-healing effect of perovskite is proved to be real [92].

Overall, perovskite materials have demonstrated good reliability in nuclear radiation environments, and their unique self-healing ability and high defect tolerance make them ideal candidates for radioisotope battery applications. Through fine compositional modulation and structural design, the energy band structure of perovskite can be further optimized to improve its ECE in radioisotope batteries. However, more tests and optimizations are still needed to address challenges such as long-term stability, temperature effects, and so forth, to realize the practical applications of perovskite radioisotope batteries.

Currently, perovskite materials in the photovoltaic industry is experiencing a critical stage from the laboratory into industrialization, perovskite head enterprises have realized the leap from megawatt to gigawatt capacity. In the field of radioisotope batteries, the economic advantages of perovskite combined with the radiation voltaic effect, an emerging nuclear energy conversion technology, due to its high energy conversion efficiency and low preparation cost, have gradually attracted attention. From the perspective of material cost as well as preparation process, the preparation of perovskite materials mainly relies on the solution method process, and the cost of its precursor is only 10% of that of crystalline silicon materials [96]. Second, the solution method process has a high material utilization rate (95%) and the equipment investment is only 30% to 50% of the traditional vacuum method. This simple and efficient preparation process corresponds to a short preparation process with low energy consumption. For example, the preparation of perovskite cells can be done at lower temperatures, while crystalline silicon cells require complex processes such as high-temperature vacuum vapor deposition. These features make the perovskite-based radioisotope batteries have significant economic advantages in large-scale production, laying the foundation for the economy of perovskite-based radioisotope batteries. And from the perspective of market potential, the flexible and lightweight characteristics of perovskite materials, which gives it a wide range of application prospects in the field of building integration, consumer electronics, and other fields. In the future, as the technology matures and the market scale expands, the economic advantages of perovskite-based radioisotope batteries will become more prominent, providing important ideas and support for the global energy transition.

6.2 | Two-Dimensional Materials Radiation Voltaic Battery

In recent years, the application of 2D materials in the field of radiation voltaic batteries has received increasing attention. Two-dimensional materials, such as graphene and molybdenum disulfide (MoS_2), show great potential due to their unique physical and chemical properties, especially in electron

transport, surface effect, and radiation response. These materials have unique advantages in radiative energy conversion, nuclear battery design, especially in terms of high efficiency energy conversion, high radiation resistance, and long lifetime. They have very high carrier mobility and electrical conductivity, which enables them to efficiently transport the charge generated by the radiation source, thus improving the ECE of the battery. The two-dimensional structure of these materials means that they have a very large specific surface area, which allows for better absorption of radiant energy during the interaction of radiation particles with the material.

Graphene, a two-dimensional material consisting of a single layer of carbon atoms, is widely used in a wide range of electronic devices and energy conversion devices by virtue of its excellent electrical and thermal conductivity and mechanical strength. Research on graphene in radiation voltaic batteries has focused on the following aspects:

Early studies found that graphene can effectively absorb radiant energy and convert it into electrical energy. The carrier mobility and electrical conductivity of graphene materials do not degrade significantly under high radiation environments, thus ensuring the stability and long life of the battery. To improve the performance of graphene-based radiation voltaic batteries, researchers have begun to compound graphene with other materials (e.g., metal oxides, MoS) to enhance their radiation responsiveness and ECE. For example, graphene composite with ZnO, TiO_2 and other materials showed strong radiation absorption and charge separation ability, researchers also optimized the electrical properties of graphene through surface modification, doping, and other methods. For example, doping N, B, and other elements can effectively change the electronic structure of graphene and improve its response to radiation energy. The application of nanomaterials and Schottky structures in radiation voltaic batteries has attracted a great deal of attention, especially the use of semi-metallic nanomaterials, such as graphene in the Schottky structure can effectively prevent carrier complexation, increase the V_{OC}, and thus improve the output performance of the battery [97]. However, the zero band gap of intrinsic graphene limits its direct application in semiconductors and microelectronics, so opening the band gap of graphene is of great significance for the research and application of graphene radiation voltaic batteries.

In 2020, Mina et al. [98] prepared a reduced graphene oxide (rGO)/Si radiation voltaic battery using reduced graphene oxide, which utilizes the potential barriers generated at the rGO/Si interface to induce an internal electric field in the Si substrate, this internal electric field can be used to separate ehp generated by β sources in Si. The current-voltage characteristics of the cell with and without radioisotope irradiation were measured using γ-Al_2O_3 with a radioactivity of 5 mCi as a source of β-radioisotope, and the V_{OC} of the cell was 34 mV, the J_{SC} was 0.41 μA cm^{-2}, and the ECE was as high as 3.9% under β-radioisotope ^{63}Ni irradiation. Han et al. [99] prepared a graphene/silicon radiation voltaic battery by using nitric acid doping and controlling the number of graphene layers. Drawing on the structure of graphene Schottky junction solar cells, the graphene/silicon Schottky junction was introduced into the radiated voltaic isotope cell to validate the feasibility of graphene/silicon Schottky junction transducer unit for the radiation voltaic battery application under irradiation of ^{63}Ni radioactive source. It is found that based on nitric acid doping, the graphene/silicon Schottky junction exchange cell obtains a V_{OC} of 48 mV and a J_{SC} of 30.3 nA cm^{-2} under irradiation of a ^{63}Ni radioactive source with an activity of 5 mCi cm^{-2}, with an ECE of about 0.1%, and its electrical output is significantly better than that of the conventional gold/silicon Schottky junction exchange cell (Figure 14d). It can be seen that the Schottky junction transduction unit using graphene as the metal electrode layer not only reduces its blocking effect on the β-particle of the radioactive source but also improves the transport effect of the electrode layer on the EHPs, compared with the conventional metal electrode.

In recent years, several research groups have successfully developed prototypes of graphene-based radiation voltaic batteries and performed performance tests. Experiments have shown that graphene-based radiation voltaic batteries are able to work stably in a prolonged radiation environment and can effectively convert radiant energy into electrical energy.

By rationally designing the composite structure of two-dimensional materials and optimizing the design of the cell, the two-dimensional material-based radiative volt effect battery is expected to achieve a high radiation energy conversion efficiency. Especially in high-energy radiation environments, the efficient energy conversion properties of 2D materials enable them to provide stable power.

Although 2D material-based radiation voltaic batteries have demonstrated significant potential in experiments, they still face several challenges: They show good stability in radiation environments, but the degradation of the materials under prolonged radiation and high temperature environments still needs to be addressed. The preparation of high-quality, high-purity materials still requires cost reductions and increased ability to scale up production. Further improvements in energy conversion efficiency and optimization of the use of materials are needed to reach commercial application levels.

7 | Summary and Outlook

As a unique energy conversion technology with the advantages of high energy density, long life and stable output, the radiation voltaic batteries are suitable for energy supply in various extreme environments. In recent years, with the development of new material technology, the performance of radiation voltaic batteries has been significantly improved. The application of wide bandwidth semiconductor materials, such as SiC, GaN and diamond, enables radiation voltaic batteries to have excellent performance under high-temperature and high-radiation environment. In addition, the introduction of perovskite and two-dimensional materials provides new possibilities for the performance enhancement of radioisotope batteries.

(1) Improvement of energy conversion efficiency and stability

Despite the remarkable progress in ECE and stability of radiation voltaic batteries, there are still some key issues that need to be addressed. First, how to further improve the ECE of the

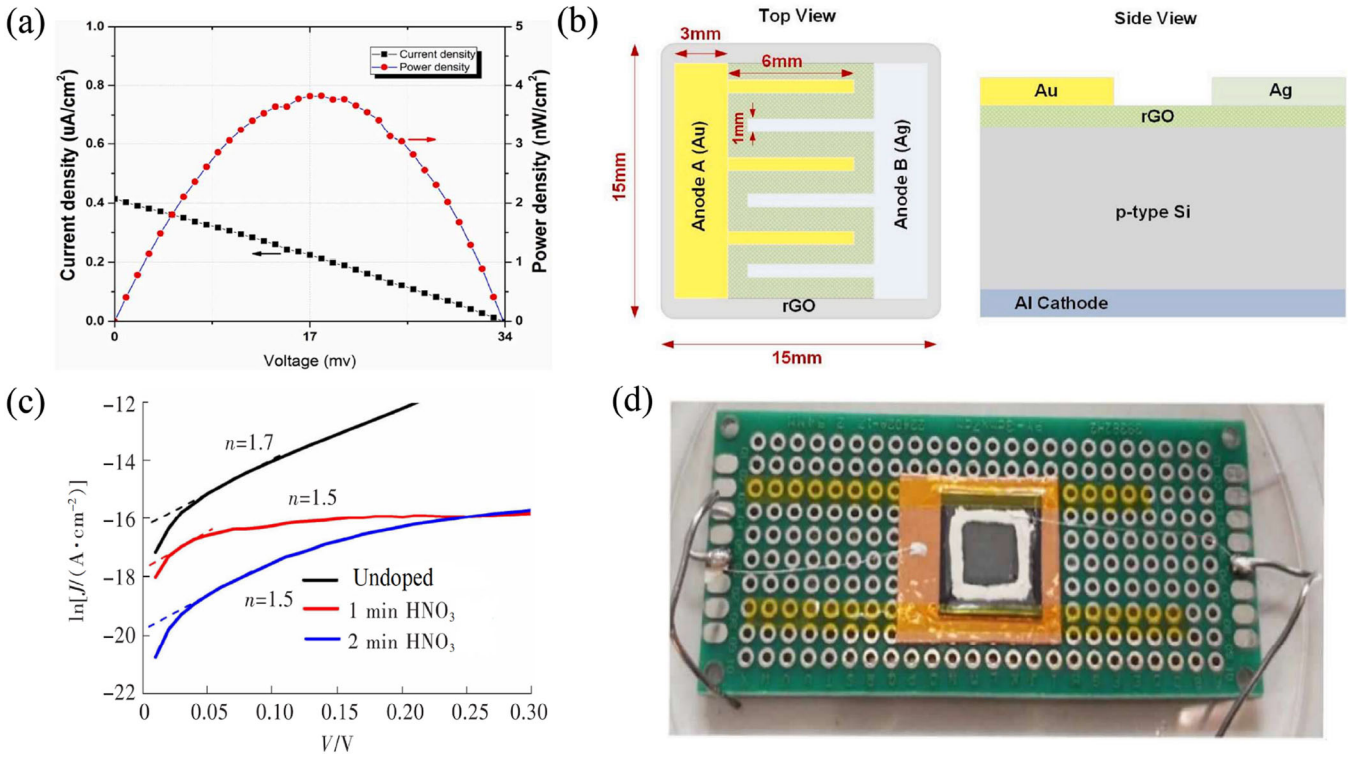

FIGURE 14 | (a) Power density and current density of rGO/Si Schottky betavoltaic cell. Reproduced with permission: Copyright 2020, Elsevier [98]. (b) Schematic representation of the energy conversion unit prepared by Mina et al. Reproduced with permission: Copyright 2020, Elsevier [98]. (c) ln *J*–*V* characteristic curves of graphene/silicon devices with different doping times of nitric acid in the dark environment. Reproduced with permission: Copyright 2019, Elsevier [99]. (d) Physical graphene/silicon Schottky junction transducing single-element device.

cell is the core issue of current research. At present, the ECE of SiC, GaN, and other wide-bandwidth semiconductor materials is close to the theoretical limit, but the efficiency in practical applications is still low. Future research can further improve the ECE of the battery by optimizing the material structure, doping process, and interface engineering. Second, the stability of the battery in a long-term high-radiation environment also needs to be further solved. Although broad-band semiconductor materials have better radiation resistance, the degradation problem of the materials still exists in extreme environments. Therefore, the development of new radiation-resistant materials or the improvement of material durability through surface passivation technology will be an important direction for future research.

(2) **Material Innovation and Structural Optimization**

Material innovation is key to advancing radiation voltaic isotope batteries. Currently, wide-bandgap semiconductors such as SiC, GaN, and diamond are widely used, but their high production costs limit large-scale applications. Future research could explore more cost-effective, high-performance semiconductor materials, such as perovskites and two-dimensional materials (e.g., graphene, MoS_2). Perovskite materials exhibit excellent optoelectronic properties and structural tunability, enabling them to effectively absorb radiant energy and convert it into electrical energy. In 2021, Li et al. fabricated high-crystallinity $MAPbBr_3$ thin films, which were used to create high-performance perovskite β-radiation voltaic cells. Under simulated β-source irradiation with a 15 keV electron beam, these cells achieved an efficiency of 5.35%. However, their stability under high-temperature and high-radiation conditions still requires further improvement. Looking ahead, perovskite radiation photovoltaic cells are expected to achieve efficiencies exceeding 6% by 2030 through bandgap engineering and heterostructure optimization and to enable continuous operation for over 10 years using defect-tolerant materials such as $CsPbBr_3$. Two-dimensional materials, with their high carrier mobility and large surface area, show great potential for radiation voltaic isotope batteries. By designing composite structures and optimizing battery layouts, these materials could achieve higher ECE.

With continuous advancements in material science, nanotechnology, and semiconductor processes, the ECE and stability of radiation voltaic isotope batteries will further improve. Future research may explore novel semiconductor materials like quantum dots, carbon nanotubes, and graphene to enhance battery efficiency. Nanotechnology enables precise control over material structures and properties, offering innovative possibilities for these batteries. Moreover, growing environmental and safety concerns are driving research toward alternative isotopes with lower radioactivity to minimize potential hazards. As the technology matures, the future may see the commercialization of radioisotope batteries in more practical applications, such as for energy supply in extreme climates, remote sensing equipment, deep ocean exploration, and long uninterrupted power supply.

In summary, radiation voltaic isotope batteries, with their unique advantages, are poised to complement traditional batteries in the near future, contributing to global energy supply and sustainable development.

Author Contributions

Qiannan Zhao: investigation, methodology, writing – original draft. **Zhenxuan Liu:** investigation, methodology, writing – original draft. **Kai Huo:** formal analysis, investigation, writing – original draft. **Wenguang Zhang:** formal analysis. **Bo Xiao:** formal analysis. **Yihuai Huang:** formal analysis. **Changkai Huang:** formal analysis. **Yao Luo:** resources. **Yan Liu:** resources. **Li Wang:** resources. **Qinghui Jiang:** methodology, resources. **Abdul Basit:** investigation, resources, writing – review and editing. **Guibin Shen:** formal analysis, investigation. **Yubo Luo:** investigation. **Xin Li:** conceptualization, investigation, writing – review and editing. **Junyou Yang:** investigation, methodology, supervision. All authors have read and agreed to the published version of the manuscript.

Acknowledgments

This study was supported by the National Natural Science Foundation of China (Grant no. 62304082), Guangdong Basic and Applied Basic Research Foundation (Grant no. 2024A1515110044), the National Key Research and Development Program of China (Grant no. 2020YFA0715000), and the Natural Science Foundation of Hubei Province (Grant no. 2023AFB087).

Conflicts of Interest

The authors declare no conflicts of interest.

References

1. C. E. Munson, Q. Gaimard, K. Merghem, et al., "Modeling, Design, Fabrication and Experimentation of a GaN-based,63Ni Betavoltaic Battery," *Journal of Physics D: Applied Physics* 51 (2018): 035101.

2. F. Urbani, G. Squadrito, O. Barbera, G. Giacoppo, E. Passalacqua, and O. Zerbinati, "Polymer Electrolyte Fuel Cell Mini Power Unit for Portable Application," *Journal of Power Sources* 169 (2007): 334–337.

3. R. Deng, B. Ke, Y. Xie, et al., "All-solid-State Thin-Film Lithium-Sulfur Batteries," *NanomicroLetters* 15, no. 1 (2023): 73.

4. M. Saravanapavanantham, J. Mwaura, and V. Bulović, "Printed Organic Photovoltaic Modules on Transferable Ultra-Thin Substrates as Additive Power Sources," *Small Methods* 7, no. 1 (2023): 2200940.

5. P. Rappaport, "The Electron-Voltaic Effect in p—n Junctions Induced by Beta-Particle Bombardment," *Physical Review* 93 (1954): 246–247.

6. L. C. Olsen, "Betavoltaic Energy Conversion," *Energy Conversion* 13 (1973): 117–127.

7. H. Guo, H. Yang, and Y. Zhang, *2007 IEEE 20th International Conference on Micro Electro Mechanical Systems (MEMS)* (IEEE, 2007), 867–870.

8. V. P. Khvostikov, V. S. Kalinovskii, S. V. Sorokina, O. A. Khvostikova, and V. M. Andreev, "Tritium Power Supply Sources Based on AlGaAs/GaAs Heterostructures," *Technical Physics Letters* 45, no. 12 (2019): 1197–1199.

9. M. V. S. Chandrashekhar, C. I. Thomas, H. Li, M. G. Spencer, and A. Lal, "Tritium Power Supply Sources Based on AlGaAs/GaAs Heterostructures," *Applied Physics Letters* 88 (2006).

10. H. Guo, Y. Shi, Y. Zhang, Y. Zhang, and J. Han, "Demonstration of a 4H SiC Betavoltaic Cell," in *2011 IEEE International Conference of Electron Devices and Solid-State Circuits* (IEEE, 2011), 1–2.

11. R. Gao, W. Ma, P. Wan, et al., "Fabrication of SiC Pin Betavoltaic Cell with 63 Ni Irradiation Source," Energy & Environmental Materials 8 (2025).

12. M. Lu, G. Zhang, K. Fu, G. Yu, D. Su, and J. Hu, "Gallium Nitride Schottky Betavoltaic Nuclear Batteries," *Energy Conversion and Management* 52 (2011): 1955–1958.

13. Z.-J. Cheng, H.-S. San, X.-Y. Chen, B. Liu, and Z.-H. Feng, "Demonstration of a High Open-Circuit Voltage GaN Betavoltaic Microbattery," *Chinese Physics Letters* 28 (2011): 078401.

14. C. E. Munson, M. Arif, J. Streque, et al., "Model of Ni-63 Battery With Realistic PIN Structure," *Journal of Applied Physics* 118, no. 10 (2015): 105101.

15. R. Gao, L. Liu, X. Xia, et al., "Isoelectronic Aluminum-Doped Gallium Nitride Alpha-Voltaic Cell With Efficiency Exceeding 4.5," *Communications Materials* 4 (2023): 50.

16. V. S. Bormashov, S. Y. Troschiev, S. A. Tarelkin, et al., "High Power Density Nuclear Battery Prototype Based on Diamond Schottky Diodes," *Diamond and Related Materials* 84 (2018): 41–47.

17. V. Bormashov, S. Troschiev, A. Volkov, et al., "Development of Nuclear Microbattery Prototype Based on Schottky Barrier Diamond Diodes," *Physica Status Solidi (a)* 212 (2015): 2539–2547.

18. X. Han, Z. Wang, F. Cao, P. Qu, P. Jin, and Z. Wang, "Diamond Schottky Barrier Diode Energy Converter Working Under~mA Output for Nuclear Batteries," *ACS Applied Electronic Materials* 6, no. 12 (2024): 8849–8854.

19. G. Li, C. Zhao, Y. Liu, et al., "High-Performance Perovskite Betavoltaics Employing High-Crystallinity $MAPbBr_3$ Films," *ACS Omega* 6 (2021): 20015–20025.

20. R. Gao, R. Chen, P. Wan, et al., "High Efficiency Formamidinium-Cesium Perovskite-Based Radio-Photovoltaic Cells," *Energy & Environmental Materials* 7, no. 1 (2024): e12513.

21. K. Li, C. Yan, J. Wang, et al., "Micronuclear Battery Based on a Coalescent Energy Transducer," *Nature* 633, no. 8031 (2024): 811–815.

22. F. K. Manasse, J. J. Pinajian, and A. N. Tse, "Schottky Barrier Betavoltaic Battery," *IEEE Transactions on Nuclear Science* 23 (1976): 860–870.

23. J. Yang, C. Fares, Y. Guan, et al., "10 MeV Proton Damage in β-Ga2O3 Schottky Rectifiers," *Journal of Vacuum Science & Technology B, Nanotechnology and Microelectronics: Materials, Processing, Measurement, and Phenomena* 36, no. 1 (2018): 011206.

24. J. Kim, S. J. Pearton, C. Fares, et al., "Radiation Damage Effects in Ga_2O_3 Materials and Devices," *Journal of Materials Chemistry C* 7 (2019): 10–24.

25. A. R. Kirmani, T. A. Byers, Z. Ni, et al., "Unraveling Radiation Damage and Healing Mechanisms in Halide Perovskites Using Energy-Tuned Dual Irradiation Dosing," *Nature Communications* 15 (2024): 696.

26. D.-Y. Qiao, X.-J. Chen, Y. Ren, and W.-Z. Yuan, "A Micro Nuclear Battery Based on SiC Schottky Barrier Diode," *Journal of Microelectromechanical Systems* 20 (2011): 685–690.

27. N. F. Mott, "The Transition to the Metallic State," *Philosophical Magazine* 6 (1961): 287–309.

28. W. G. Pfann and W. Van Roosbroeck, "Radioactive and Photoelectricp-Njunction Power Sources," *Journal of Applied Physics* 25 (1954): 1422–1434.

29. M. Lewis and S. E. Seeman, "Performance Experience With Prototype Betacel Nuclear Batteries," *Nuclear Technology* 17 (1973): 160–167.

30. L. C. Olsen, Lewis Research Center, "Review of Betavoltaic Energy Conversion," in *Proceedings of the 12th Space Photovoltaic Research and Technology Conference (SPRAT 12)* (NASA, 1993), 256–267.

31. P. Liu, Y. Chang, and J. Zhang, "Single-Walled Carbon Nanotube Film-Silicon Heterojunction Radioisotope Betavoltaic Microbatteries," *Journal of Micromechanics and Microengineering* 24 (2014): 055026.

32. X. Tang, D. Ding, Y. Liu, and D. Chen, "Optimization Design and Analysis of Si-^{63}Ni Betavoltaic Battery," *Science China: Technological Sciences* 55 (2012): 990–996.

33. K. Wu, C. Dai, and H. Guo, "A theoretical Study on Silicon Betavoltaics Using Ni-63," in *2011 6th IEEE International Conference on Nano/Micro Engineered and Molecular Systems* (IEEE, 2011), 724–727.

34. J. Chu, "Research of Radioisotope Microbattery Based on β-radio-Voltaic Effect," *Journal of Micro/Nanolithography, MEMS, and MOEMS* 8 (2009): 021180.

35. J. Wang, P. Jin, P. L. Bishop, and F. Li, "Upgrade of Three Municipal Wastewater Treatment Lagoons Using a High Surface Area Media," *Frontiers of Environmental Science & Engineering* 6 (2012): 288–293.

36. L. Sun, W. Yuan, D. Qiao, and C. Qin, "Design and Simulation of a Novel Radioisotope Micro Battery Based on MEMS," *Chinese Journal of Sensors and Actuators* 19 (2006): 997–1000.

37. S. Deus, "Tritium-Powered Betavoltaic Cells Based on Amorphous Silicon," in *Conference Record of the Twenty-Eighth IEEE Photovoltaic Specialists Conference-2000* (Cat. No.00CH37036), (IEEE, 2000), 1246–1249.

38. J. Blanchard, D. Henderson, and A. Lal, Nuclear Microbattery for MEMS Devices, Nasa Sti/Recon Technical Report N (2001): 3.

39. H. Guo and A. Lal, "TRANSDUCERS '03," in 12th International Conference on Solid-State Sensors, Actuators and Microsystems. Digest of Technical Papers (Cat. No.03TH8664), (IEEE, 2003), 36–39.

40. J. Guo, X. Liu, J. Yu, et al., "An Overview of The Comprehensive Utilization of Silicon-Based Solid Waste Related to PV Industry," *Resources, Conservation and Recycling* 169 (2021): 105450.

41. L. Shen, S. Li, Y. Wang, et al., "Upcycling Photovoltaic Silicon Waste Into Cost-Effectiveness Si/C Anode Materials," *Carbon Energy* 7, no. 7 (2025): e70004.

42. J. Lu, J. Liu, X. Gong, et al., "Upcycling of Photovoltaic Silicon Waste Into Ultrahigh Areal-Loaded Silicon Nanowire Electrodes Through Electrothermal Shock," *Energy Storage Materials* 46 (2022): 594–604.

43. L. Shen, K. Sun, F. Xi, et al., "Conversion of Photovoltaic Waste Silicon Into Amorphous Silicon Nanowire Anodes," *Energy & Environmental Science* 18 (2025): 4348–4361.

44. J. Lu, S. Liu, J. Liu, et al., "Millisecond Conversion of Photovoltaic Silicon Waste to Binder-Free High Silicon Content Nanowires Electrodes," *Advanced Energy Materials* 11, no. 40 (2021): 2102103.

45. H. Flicker, J. J. Loferski, and T. S. Elleman, "Construction of a Promethium-147 Atomic Battery," *IEEE Transactions on Electron Devices* 11 (1964): 2–8.

46. G. N. Yakubova, *Urbana* (University of Illinois, 2010).

47. H. Chen, L. Jiang, and X. Chen, "Design Optimization of GaAs Betavoltaic Batteries," *Journal of Physics D: Applied Physics* 44 (2011): 215303.

48. R. Zheng, J. Lu, Y. Wang, et al., "Enhanced Performance of GaAs-Based Betavoltaic Batteries by Using AlGaAs Hole/Electron Transport Layers," *Journal of Physics D: Applied Physics* 55 (2022): 304002.

49. M. V. Dorokhin, O. V. Vikhrova, P. B. Demina, et al., "GaAs Diodes for TiT_2-based Betavoltaic Cells," *Applied Radiation and Isotopes* 179 (2022): 110030.

50. D.-R. Li, L. Jiang, J.-H. Yin, Y.-Y. Tan, and N. Lin, "Betavoltaic Battery Conversion Efficiency Improvement Based on Interlayer Structures," *Chinese Physics Letters* 29 (2012): 078102.

51. S. Butera, G. Lioliou, and A. M. Barnett, "Temperature Effects on Gallium Arsenide 63 Ni Betavoltaic Cell," *Applied Radiation and Isotopes* 125 (2017): 42–47.

52. V. M. Andreev, A. G. Kevetsky, V. S. Kaiinovsky, et al., "Tritium-Powered Betacells Based on $Al_xGa_{1-x}As$," in *Conference Record of the Twenty-Eighth IEEE Photovoltaic Specialists Conference-2000* (Cat. No.00CH37036) (IEEE, 2000), 1253–1256.

53. L. Fu, J. Li, G. Wang, Y. Luan, and W. Dai, "Adsorption Behavior of Organic Pollutants on Microplastics," *Ecotoxicology and Environmental Safety* 217 (2021): 112207.

54. C. Qian, H. Guo, C. Han, H. Yuan, Y. Zhang, and Y. Zhang, "Design of High-Efficiency SiC Betavoltaic Battery Structures With Reduced Impact of Near-Surface Recombination Based on Accurate Modeling," *IEEE Transactions on Electron Devices* 69 (2022): 7141–7146.

55. X. Y. Li, Y. Ren, X. J. Chen, D. Y. Qiao, and W. Z. Yuan, "63Ni Schottky Barrier Nuclear Battery of 4H-SiC," *Journal of Radioanalytical and Nuclear Chemistry* 287 (2011): 173–176.

56. C. Thomas, S. Portnoff, and M. G. Spencer, "High Efficiency 4H-SiC Betavoltaic Power Sources Using Tritium Radioisotopes," *Applied Physics Letters* 108, no. 1 (2016): 013505.

57. R. Zheng, J. Lu, Y. Liu, et al., "Comparative Study of GaN Betavoltaic Battery Based on pn Junction and Schottky Barrier Diode," *Radiation Physics and Chemistry* 168 (2020): 108595.

58. M. G. Cheong, K. S. Kim, C. S. Oh, et al., "Conductive Layer Near the GaN/Sapphire Interface and Its Effect on Electron Transport in Unintentionally Doped n-Type GaN Epilayers," *Applied Physics Letters* 77 (2000): 2557–2559.

59. D. C. Look and R. J. Molnar, "Degenerate Layer at GaN/Sapphire Interface: Influence on Hall-Effect Measurements," *Applied Physics Letters* 70 (1997): 3377–3379.

60. Z. Cheng, X. Chen, H. San, Z. Feng, and B. Liu, "A High Open-Circuit Voltage Gallium Nitride Betavoltaic Microbattery," *Journal of Micromechanics and Microengineering* 22 (2012): 074011.

61. A. Toprak, D. Yılmaz, and E. Özbay, "A Study on GaN-Based Betavoltaic Batteries," *Semiconductor Science and Technology* 37 (2022): 125005.

62. M. T. Noman, M. A. Ashraf, and A. Ali, "Synthesis and Applications of nano-TiO_2: A Review," *Environmental Science and Pollution Research* 26 (2019): 3262–3291.

63. A. M. Ruiz, G. Sakai, A. Cornet, K. Shimanoe, J. R. Morante, and N. Yamazoe, "Microstructure Control of Thermally Stable TiO_2 Obtained by Hydrothermal Process for Gas Sensors," *Sensors and Actuators B: Chemical* 103 (2004): 312–317.

64. C. He, X. Z. Li, N. Graham, and Y. Wang, "Preparation of TiO_2/ITO and TiO_2/Ti Photoelectrodes by Magnetron Sputtering for Photocatalytic Application," *Applied Catalysis, A: General* 305 (2006): 54–63.

65. K. Lee, A. Mazare, and P. Schmuki, "One-Dimensional Titanium Dioxide Nanomaterials: Nanotubes," *Chemical Reviews* 114 (2014): 9385–9454.

66. N. Wang, Y. Ma, J. Chen, et al., "Defect-Induced Betavoltaic Enhancement in Black Titania Nanotube Arrays," *Nanoscale* 10 (2018): 13028–13036.

67. Y. Ma, N. Wang, J. Chen, et al., "Betavoltaic Enhancement Using Defect-Engineered TiO_2 Nanotube Arrays Through Electrochemical Reduction in Organic Electrolytes," *ACS Applied Materials & Interfaces* 10 (2018): 22174–22181.

68. J.-Y. Lee, J. Park, and J.-H. Cho, Applied Physics Letters 87, no. 1 (2005): 011904.

69. E. L. Boytsova, L. A. Leonova, and V. F. Pichugin, "The Structure of Biocoats Based on TiO_2 Doped With Nitrogen Study," *IOP Conference Series: Materials Science and Engineering* 347 (2018): 012025.

70. C. Li, Y. Hsieh, W. Chiu, C. Liu, and C. Kao, "Study on Preparation and Photocatalytic Performance of Ag/TiO_2 and Pt/TiO_2 Photocatalysts," *Separation and Purification Technology* 58 (2007): 148–151.

71. Z. Ding, T.-X. Jiang, R.-R. Zheng, et al., "Quantitative Modeling, Optimization, and Verification of ^{63}Ni-Powered Betavoltaic Cells Based on Three-Dimensional ZnO Nanorod Arrays," *Nuclear Science and Techniques* 33 (2022): 144.

72. Z. Movahedian and H. Tavakoli-Anbaran, "Experimental and Theoretical Study of ^{90}Sr/^{90}Y-n-Si/ZnO Betavoltaic Battery and Theoretical Prediction of Homojunction Betavoltaic Cells Performance," *Materials Science in Semiconductor Processing* 186 (2025): 109059.

73. M. Maghsodi and H. Tavakoli-Anbaran, "ZnO Betavoltaic Batteries: Exploring Cylindrical Designs for Maximum Efficiency and Output," *Arabian Journal for Science and Engineering* 50 (2025): 1–15.

74. Z. Movahedian and H. Tavakoli-Anbaran, "Exploratory Study of Betavoltaic Nuclear Battery Using AlN PN Junction," *Journal of Energy Storage* 72 (2023): 108485.

75. B. Liu, K. Liu, V. Ralchenko, et al., "Effect of Americium-241 Source Activity on Total Conversion Efficiency of Diamond Alpha-Voltaic Battery," *International Journal of Energy Research* 43 (2019): 6038–6044.

76. B. Liu, K. Liu, J. Zhao, et al., "Enhanced Performance of Diamond Schottky Nuclear Batteries by Using ZnO as Electron Transport Layer," *Diamond and Related Materials* 109 (2020): 108026.

77. Shivani, D. Kaur, A. Ghosh, and M. Kumar, "A Strategic Review on Gallium Oxide Based Power Electronics: Recent Progress and Future Prospects," *Materials Today Communications* 33 (2022): 104244.

78. Z. Wang, G. Zhang, X. Zhang, et al., "Polarization-Sensitive Artificial Optoelectronic Synapse Based on Anisotropic β-Ga_2O_3 Single Crystal for Neuromorphic Vision Systems and Information Encryption," *Advanced Optical Materials* 12, no. 29 (2024): 2401256.

79. C. Wu, F. Wu, H. Hu, S. Wang, A. Liu, and D. Guo. "Review of Self-Powered Solar-Blind Photodetectors Based on Ga_2O_3," *Materials Today Physics* 28 (2022): 100883.

80. M. R. Lorenz, J. F. Woods, and R. J. Gambino, "Some Electrical Properties of the Semiconductor β-Ga_2O_3," *Journal of Physics and Chemistry of Solids* 28 (1967): 403–404.

81. N. Ma, N. Tanen, A. Verma, et al., "Intrinsic Electron Mobility Limits in β-Ga_2O_3," *Applied Physics Letters* 109, no. 21 (2016): 212101.

82. M. Higashiwaki, H. Murakami, Y. Kumagai, and A. Kuramata, "Current Status of Ga_2O_3 Power Devices," *Japanese Journal of Applied Physics* 55 (2016): 1202A1.

83. S. J. Pearton, J. Yang, P. H. Cary, et al., "A Review of Ga_2O_3 Materials, Processing, and Devices," *Applied Physics Review* 5, no. 1 (2018): 011301.

84. J. Zhang, J. Willis, Z. Yang, et al., "Direct Determination of Band-Gap Renormalization in Degenerately Doped Ultrawide Band Gap β-Ga_2O_3 Semiconductor," *Physical Review B* 106 (2022): 205305.

85. M. A. Mastro, A. Kuramata, J. Calkins, J. Kim, F. Ren, and S. J. Pearton, "Perspective—Opportunities and Future Directions for Ga_2O_3," *ECS Journal of Solid State Science and Technology* 6 (2017): P356–P359.

86. X. Liu, S. Lu, and M. Xia, "Advances in High-Energy Irradiation Stability and Damage Mechanisms of Perovskite Materials," *Chin J Lum* 46 (2025): 642–657.

87. W. Chen, Y. Liu, Z. Yuan, et al., "X-Ray Radioluminescence Effect of All-Inorganic Halide Perovskite $CsPbBr_3$ Quantum Dots," *Journal of Radioanalytical and Nuclear Chemistry* 314 (2017): 2327–2337.

88. W. Chen, X. Tang, Y. Liu, et al., "Novel Radioluminescent Nuclear Battery: Spectral Regulation of Perovskite Quantum Dots," *International Journal of Energy Research* 42 (2018): 2507–2517.

89. Z. Xu, X. Tang, Y. Liu, et al., "$CsPbBr_3$ Quantum Dot Films With High Luminescence Efficiency and Irradiation Stability for Radioluminescent Nuclear Battery Application," *ACS Applied Materials & Interfaces* 11 (2019): 14191–14199.

90. Z. Xu, Y. Liu, and X. Tang, "Radioluminescent Nuclear Battery Technology Development for Space Exploration," *Advances in Astronautics Science and Technology* 3 (2020): 125–131.

91. W. Xiong, W. Tang, G. Zhang, et al., "Controllable p- and n-Type Behaviours in Emissive Perovskite Semiconductors," *Nature* 633 (2024): 344–350.

92. V. Milotti, S. Cacovich, D. R. Ceratti, et al., "Degradation and Self-Healing of $FAPbBr_3$ Perovskite Under Soft-X-Ray Irradiation," *Small Methods* 7, no. 9 (2023): 2300222.

93. Z. Liao, Z. Xiao, M. Yang, et al., "Direct Imaging of Carrier Diffusion Length in Organic-Inorganic Perovskites," *Applied Physics Letters* 115, no. 24 (2019): 242104.

94. J. Ding, Z. Lian, Y. Li, S. Wang, and Q. Yan, "The Role of Surface Defects in Photoluminescence and Decay Dynamics of High-Quality Perovskite $MAPbI_3$ Single Crystals," *Journal of Physical Chemistry Letters* 9 (2018): 4221–4226.

95. R. Li, B. Li, X. Fang, et al., "Self-Structural Healing of Encapsulated Perovskite Microcrystals for Improved Optical and Thermal Stability," *Advanced Materials* 33, no. 21 (2021): 2100466.

96. Q. Li, Y. Zheng, H. Wang, et al., "Graphene-Polymer Reinforcement of Perovskite Lattices for Durable Solar Cells," *Science* 387 (2025): 1069–1077.

97. Y. Naghipour and M. Amirmazlaghani, "Graphene/Porous GaN Schottky Betacell," *Micro and Nanostructures* 168 (2022): 207323.

98. M. Amirmazlaghani, A. Rajabi, Z. Pour-mohammadi, and A. A. Sehat, "Betavoltaic Battery Based on Reduced-Graphene-Oxide/Si Heterojunction," *Superlattices and Microstructures* 145 (2020): 106602.

99. X. Wang, Y. Han, J. Zhang, et al., "The Design of a Direct Charge Nuclear Battery With High Energy Conversion Efficiency," *Applied Radiation and Isotopes* 148 (2019): 147–151.